

AGROCAMPUS OUEST

CFR Angers CFR Rennes

<p>Année universitaire : 2020 - 2021</p> <p>Spécialité :</p> <p>Ingénieur Agronome</p> <p>Spécialisation (et option éventuelle) :</p> <p>Sciences halieutiques et aquacoles (Ressources et Ecosystèmes Aquatiques)</p>	<p>Mémoire de fin d'études</p> <p><input checked="" type="checkbox"/> d'ingénieur d'AGROCAMPUS OUEST (École nationale supérieure des sciences agronomiques, agroalimentaires, horticoles et du paysage), école interne de L'institut Agro (Institut national d'enseignement supérieur pour l'agriculture, l'alimentation et l'environnement)</p> <p><input type="checkbox"/> de master d'AGROCAMPUS OUEST (École nationale supérieure des sciences agronomiques, agroalimentaires, horticoles et du paysage), école interne de L'institut Agro (Institut national d'enseignement supérieur pour l'agriculture, l'alimentation et l'environnement)</p> <p><input type="checkbox"/> de Montpellier SupAgro (étudiant arrivé en M2)</p> <p><input type="checkbox"/> d'un autre établissement (étudiant arrivé en M2)</p>
--	--

**SPATIAL AND INTER-ANNUAL VARIABILITY GRADIENTS OF
ZOOPLANKTONIC TAXONOMIC AND FUNCTIONAL DIVERSITY IN THE
GULF OF LIONS**

Par Amélie NITHARD

Soutenu à RENNES le 16 septembre 2021

Devant le jury composé de :

Président : Olivier LE PAPE

Maître de stage 1 : Tarek HATTAB

Maître de stage 2 : Dorothée VINCENT

Enseignant référent : Olivier LE PAPE

Autres membres du jury (Nom, Qualité)

Etienne RIVOT (Enseignant-chercheur, Agrocampus Ouest)

Pablo Brosset (Chercheur, IFREMER Brest)

Les analyses et les conclusions de ce travail d'étudiant n'engagent que la responsabilité de son auteur et non celle d'AGROCAMPUS OUEST

Ce document est soumis aux conditions d'utilisation

« Paternité-Pas d'Utilisation Commerciale-Pas de Modification 4.0 France »

disponible en ligne <http://creativecommons.org/licenses/by-nc-nd/4.0/deed.fr>



REMERCIEMENTS

Je tiens tout d'abord à remercier Tarek et Dorothée, mes deux encadrants, qui ont toujours été disponibles et joignables, et cela même pendant leurs congés. Merci pour votre super encadrement et toute l'aide que vous m'avez apportée, et ce jusqu'à la dernière seconde. Vraiment merci beaucoup.

Je souhaiterai également remercier toute l'équipe PELMED et l'équipage de l'Europe. C'était mon premier embarquement sur une campagne scientifique et malgré les quelques aléas lors de mes legs, j'ai vraiment passé une expérience inoubliable. Un spécial merci à Leelou, ma colocataire de cabine lors de cette aventure.

Pour finir je remercie Judith, ma colocataire lors de ces 6 mois à Sète qui tous les jours rentrait avec une nouvelle histoire à me raconter. Cela égayait mes journées, merci.

1- INTRODUCTION	1
1.1. Plankton: definition and general description	1
1.2. Plankton and marine food-webs	1
1.3. Zooplankton as indicators of environmental changes at different scales: link with European directives	2
1.4. Study site and objectives of the internship	3
2. MATERIALS AND METHODS	4
2.1- Data collection	4
2.1.1- PELMED sampling design	4
2.1.2- Environmental data	5
2.1.2.1- In situ data from PELMED surveys	6
2.1.2.2- Satellite data	7
2.1.3- Zooplankton data	8
2.2- Building a zooplankton functional traits database	8
2.2.1- Harmonization/homogenization of available data	8
2.2.2- Data selection	9
2.2.3- Zooplankton functional traits	9
2.3- Data analyses	11
2.3.1- Exploratory analyses	11
2.3.2- Mapping in situ and satellite derived data	12
2.3.3- Functional traits: community weighted mean	13
2.3.4- Ecological and environmental indicators	14
2.3.4.1 Environmental turnover	14
2.3.4.2- Spatial and temporal variability of the alpha taxonomic diversity	14
2.3.4.3- Beta functional diversity	15
3. RESULTS	16
3.1- Interannual and spatial variability of environmental conditions	16
3.2- Interannual and spatial variability of copepod communities	20
3.2.1. Total copepods abundance	20
3.2.2. Copepod assemblages: composition and interannual variability	20
3.2.3- Copepod diversity	21
3.2.3.1 - Alpha diversity: Simpson index	21
3.2.3.2 - Functional beta diversity	23
3.2.3.3 - Relating copepod functional traits to environmental conditions	26
4. DISCUSSION	28
4.1- Methodological considerations	28
4.1.1. - PELMED sampling design and impact on environmental and zooplankton dataset	28
4.1.2. - Zooplankton functional traits definition	29
4.2- Summer environmental conditions during PELMED surveys over the period 2013-2019	30

4.3- Summer copepod communities: composition, functional diversity and spatial and interannual variability	31
4.3.1. - Structure of summer zooplankton communities	31
4.3.2. - Copepods spatial variability during summer	32
4.3.3. Copepod functional traits and environment relationships	33
5. CONCLUSION AND MONITORING PERSPECTIVES	34
REFERENCES	36
APPENDICES	41

List of tables

Table I: Number of CTD casts and zooplankton samples collected (WP2 net) each year during PELMED surveys.....	5
Table II. Functional traits derived from Benedetti et al. (2016)* and Brun et al. (2016)**.....	10
Table III: Summary of the CWM RDA	28

List of the figures

Figure 1. location of sampling stations during PELMED surveys from 2013 to 2019.....	5
Figure 2: Relative abundance of dominant plankton groups from 2013-2019 during PELMED surveys.....	9
Figure 3: Steps of the database construction for copepod functional traits	11
Figure 4. Illustration of the block averaging method principle as described in Masse et al. (2018)	13
<i>Figure 5: Map of mean Sea surface temperature (SST; °C) derived from satellite data (CMEMS data) during PELMED surveys from 2013 to 2019</i>	<i>16</i>
<i>Figure 6: Map of salinity at the surface (PSU) collected during PELMED surveys from 2013 to 2019</i>	<i>17</i>
<i>Figure 7: Wind Rose (direction and speed in $m s^{-1}$) during PELMED surveys from 2013 to 2019</i>	<i>17</i>
<i>Figure 8: map of the potential energy deficit calculated from the PELMED surveys data from 2013 to 2019</i>	<i>18</i>
<i>Figure 9: map of chl-a concentration ($mg.m^{-3}$) during PELMED surveys data from 2013 to 2019</i>	<i>18</i>
Figure 10: Spatial and temporal projection of PCoA axes of environmental data	19
Figure 11: Map of total copepod abundance ($ind m^{-3}$) during PELMED surveys from 2013 to 2019	20
<i>Figure 12: Barplot showing the relative abundance of the main copepod species in the gulf of Lion and their interannual variability</i>	<i>21</i>
<i>Figure 13: Simpson Index of copepod during PELMED surveys from 2013 to 2019</i>	<i>22</i>
<i>Figure 14: Pielou Index of copepod during PELMED surveys from 2013 to 2019</i>	<i>22</i>
<i>Figure 15: Maps of the functional trait “max length” (mm) during PELMED survey from 2013 to 2019</i>	<i>23</i>
<i>Figure 16: Maps of the Omnivorous-Herbivorous copepods during PELMED survey from 2013 to 2019</i>	<i>24</i>
<i>Figure 17: Maps of the active ambush feeders during PELMED survey from 2013 to 2019</i>	<i>24</i>
<i>Figure 18: Maps of the epipelagic copepods during PELMED survey from 2013 to 2019</i>	<i>25</i>
Figure 19: Spatial and temporal projection of RDA axes	26
Figure 20: CWM-RDA axes and environmental variables correlation	27

List of Appendices

APPENDIX 1 Table : Review of kriging methods (principle, pros and cons) tested to map copepod abundance from PELMED surveys	42
APPENDIX 2: Maps of wind speed in July in m.s-1 during PELMED survey from 2013 to 2019.....	44
APPENDIX 3: Maps of turbidity in mg.m-3 during PELMED survey from 2013 to 2019.....	45
APPENDIX 4: Map of abundance (ind.m ⁻³) of <i>Acartia clausi</i> during PELMED surveys from 2013 to 2019.....	46
APPENDIX 5: Map of abundance (ind.m ⁻³) of <i>Centropages typicus</i> during PELMED surveys from 2013 to 2019.....	47
APPENDIX 6: Map of abundance (ind.m ⁻³) of <i>Oithona similis</i> during PELMED surveys from 2013 to 2019.....	48
APPENDIX 7 : Simpson diversity index of copepod during PELMED surveys from 2013 to 2019	49
APPENDIX 8: Species richness index during PELMED surveys from 2013 to 2019	50
APPENDIX 9: Map of abundance (ind.m ⁻³) of <i>Heterorhabdus pappiliger</i> during PELMED surveys from 2013 to 2019	51
APPENDIX 10: Map of abundance (ind.m ⁻³) of <i>Pleurommama gracilis</i> during PELMED surveys from 2013 to 2019	52
APPENDIX 11: Map of abundance (ind.m ⁻³) of <i>Nannocalanus minor</i> during PELMED survey from 2013 to 2019.....	53
APPENDIX 12: Map of abundance (ind.m ⁻³) of <i>Oithona nana</i> during PELMED surveys from 2013 to 2019	54
APPENDIX 13: Map of abundance (ind.m ⁻³) of <i>Oithona plumifera</i> during PELMED surveys from 2013 to 2019.....	55
APPENDIX 14: Map of abundance (ind.m ⁻³) of <i>Oithona setigera</i> during PELMED surveys from 2013 to 2019.....	56
APPENDIX 15:Map of abundance (ind.m ⁻³) of <i>Diaxis pygmea</i> during PELMED survey from 2013 to 2019.....	57
APPENDIX 16: Map of abundance (ind.m ⁻³) of <i>Haloptilus longicornis</i> during PELMED survey from 2013 to 2019.....	58

1- INTRODUCTION

1.1- Plankton: definition and general description

Plankton refers to drifting organisms living in the water column and whose motion is mainly determined by hydrodynamics (e.g., currents tides). Plankton organisms cover a wide range of sizes (from nanometre to centimetre) comprise a large diversity of forms, shapes and taxa (e.g. from bacteria to jellyfish), of behaviours (feeding, migration, reproduction,), life cycles (meroplankton i.e. planktonic during part of their lives versus holoplankton i.e. spend their entire life as part of the plankton) and diets (e.g. autotrophic, heterotrophic, mixotrophic).

1.2 - Plankton and marine food-webs

Plankton is the foundation of the marine food web, more specifically phytoplankton, which is considered as the main energy source of the pelagic ecosystems. Indeed, 45% of the annual primary production of the earth is provided by phytoplankton (Field et al., 1998). Via photosynthesis, phytoplankton play an essential role in carbon sequestration and assimilation in the oceans, regulating the planet climate (Raven and Falkowski, 1999). The entire marine food web is dependent on phytoplankton. Indeed, herbivorous zooplankton which are considered as secondary producers, feed on phytoplankton, and occupy a pivotal position between primary producers and small planktivorous predators such as pelagic fishes larvae (Fransz et al., 1991). Some of these most important intermediates are copepods, being the most prominent zooplankton and therefore playing a major role in trophic flux transfer (Schminke, 2007; Richardson, 2008). However, though copepods were long thought to be strictly herbivorous, the flexibility of their diet was demonstrated a number of times since the 1980s. Copepods were in fact demonstrated to graze on microbial components (e.g. ciliates and dinoflagellates; Stoecker and Egloff, 1987), detritus (Roman, 1984), aggregates (Lombard et al., 2013) and fecal pellets (Poulsen and Kiørboe, 2005); review by Turner, 2015). They are therefore qualified as omnivorous feeders, being able to modify their diet composition according to prey size (Hansen et al., 1994), prey biogeochemical composition (Hassett, 2004) and prey standing stocks (Garrido et al., 2013; Helenius and Saiz, 2017). Plankton communities exert bottom-up control on the trophic web and this control can, to some extent, lead to changes in fish recruitment (Beaugrand, 2003) and in regime shift i.e. a sudden shift in structure and functioning of a marine ecosystem, affecting several living components and resulting in an alternate state (Cury and Shannon, 2004). Several studies have indeed shown that a decrease in primary production can affect the entire food web. For example, Beaugrand et al. (2003) provided evidence that the cod recruitment in the North Sea is either decreasing or increasing depending on changes in plankton community. In the Pacific ocean, Ware and Thomson, (2005) linked water warming to the decrease in zooplankton biomass and hence, to the recent downward trend in fish population in the region.

As plankton community variability in composition and standing stocks can impact higher trophic levels, it appears necessary to clearly identify how communities respond to environmental changes and therefore, to consider different scales of observations.

1.3- Zooplankton as indicators of environmental changes at different scales: link with European directives

Zooplankton species largely depend on ocean conditions (Richardson and Schoeman, 2004; Beaugrand and Kirby, 2010). Particularly sensitive to subtle hydro-meteorological changes (Goberville et al., 2014), they integrate and transfer environmental signals over generation time (Richardson, 2008). Consequently, zooplankton species are known to mirror ecosystems conditions and their changes over space and time. Modification in community composition, structure and/or abundance is hence often related to rapid and major alterations of ecosystem structure (Nicolas et al., 2014). In addition, plankton are good integrators and sometimes they can be amplifiers of the environmental conditions and the changes that occur at longer scales (e.g. decades; Hayes et al., 2005; Beaugrand and Kirby, 2010; Bedford et al., 2020). Some evidence suggests that plankton are more sensitive indicators of change than even environmental variables themselves, because the non-linear responses of plankton communities can amplify subtle environmental signals (Taylor, 2002). Hence, they are considered as good indicators of environmental changes for several reasons. First, most zooplankton species are not commercially exploited, so if any long-term changes stand out, the main explanation would be the environmental changes, and not due to direct exploitation (Hayes et al., 2005). Second, nearly all zooplankton species have a short life span, so the persistence of individuals from previous years have less influence on the current population (Hayes et al., 2005). Third, due to the floating characteristic of zooplankton, they rapidly reflect the effects of water quality (e.g. temperature changes, nutrient enrichment resulting in phytoplankton growth) and ocean currents, therefore their distribution and composition reflect these environmental conditions by changing dramatically (Hayes et al., 2005; Richardson, 2008).

As good environmental indicators, plankton communities can be used to monitor marine ecosystems. Within the EU Marine Strategy Framework Directive (MSFD, 2008/56/EC- European Commission, 2008), "Pelagic Habitats" are a part of the D1-Biodiversity thematic programme for which the aim stated by the EU is "*Biological diversity is maintained. The quality and occurrence of habitats and the distribution and abundance of species are in line with prevailing physiographic, geographic and climatic conditions*". To answer this objective, The French Ministry of Ecology defined a Pelagic Habitats (PelHab) monitoring programme. This monitoring programme aims to acquire relevant data allowing to assess periods and sites at stake regarding plankton communities (i.e., phytoplankton, zooplankton and micro-organisms). In a nutshell, the implementation of the monitoring programme goes through the characterization of plankton communities in an integrative manner (phyto-, zooplankton and micro-organisms), their composition, distribution, and variability in relation to associated environmental conditions (hydroclimatic conditions, physico-chemistry and biology). The PelHab monitoring programme concerns the territorial French waters from coastal waters to offshore waters (limited by the Exclusive Economic Zone, EEZ). It relies on existing monitoring surveys that were defined in the frame of existing directives (e.g. the common fishery policy, CFP) as well as on existing monitoring programmes developed for research activities and ocean observation (SOMLIT¹; MOOSE²). As most of the existing surveys cover the coastal area (< 12 nautical mile), data acquisition

¹ Service d'Observation du Milieu Littoral

² Mediterranean ocean observing system for the environment

offshore is completed by additional methods such as satellite derived products and modelling. However, though these tools are totally operational to provide relevant data offshore, the type of data acquired mainly concern hydrology (sea surface temperature), physico-chemical parameters (turbidity and nutrients via models) and phytoplankton. In addition, satellite and coupled hydrodynamical - biogeochemical models must be routinely validated by *in situ* data. It was therefore important to deploy new operational and standardized surveys to collect the data needed to assess the state of the marine environment within offshore ecosystems. To this end, surveys existing within the CFP were optimized and adapted to the needs of MSFD Pel Hab monitoring programme (Baudrier et al., 2018). This avoided creating new surveys which would have been costly and time consuming. Six shipborne surveys, related to the requirements of the European data collection framework (DCF), are used for the purposes of the MSFD French legislation: IBTS (<https://doi.org/10.18142/17>), PELGAS (<https://doi.org/10.18142/18>) in the Channel - North Sea French region, MEDITS (<https://doi.org/10.18142/7>), PELMED in the Western Mediterranean Sea, CGFS (<https://doi.org/10.18142/19>) and EVHOE (<https://doi.org/10.18142/8>) in the Bay of Biscay and Celtic Seas regions.

However and though these surveys were identified as relevant data providers for the assessment of the good environmental status of Pelagic Habitats, data were not exploited so far since (i) acquisition frequency (twice a year) is incompatible with Pelagic Habitats indicators computation which requires monthly data and (ii) data acquisition was initiated at distinct dates according to surveys (e.g. 2013 for PELMED, 2018 for EVHOE) and plankton component considered (phytoplankton, zooplankton) as the optimisation phase necessitated sampling tests onboard. Therefore, data were not exploited though it is an absolute prerequisite to infer the relevance of this data regarding PelHab monitoring programme, especially given the 2nd 6-year-cycle of MSFD monitoring programmes has been launched in 2021.

1.4 - Study site and objectives of the internship

PELMED surveys allow the acquisition of summer plankton data (phyto- and zooplankton) at large scale down to the species level since 2013 in the Gulf of Lion (GoL, North-western Mediterranean Sea; between 42° 15' N and 43° 35' N and 3° 00' E and 6° 00' E) and were therefore chosen as the main focus of this internship.

The area covered by the GoL is approximately 15 000 km² and is characterized by a 80 km wide continental shelf where complex hydrological dynamics processes occur. Hydrodynamics is influenced by shallow water depths of the shelf, wind regimes (Mistral and Tramontane), the Northern Current (NC), and freshwater inputs from the Rhône River (Gatti et al., 2006; Fraysse et al., 2014). A high seasonal variability also characterizes hydrodynamic features : while a decrease in NC intensity is observed in summer, it becomes faster, deeper and narrower in winter (Millot, 1990). Besides, the mean flux of the Rhone River is the highest into the north-western Mediterranean area, reaching almost 1700 m³.s⁻¹ (Millot, 1990) and being responsible for 95% of suspended particulate matter flux to the French Mediterranean coast (Sadaoui et al., 2016). Due to this important discharge, the GoL is one of the most productive areas of the Mediterranean Sea, the Rhone River discharge contributing up to 50% of the GoL primary production (Lochet and Leveau, 1990). This productive shelf is also highly exploited for commercial fishing (Bănaru et al., 2013) and the coastal area is strongly influenced by tourism activities.

Significant changes have recently occurred in the pelagic ecosystem of the Gulf of Lion, such as decrease of nutrient concentrations from east to west and from coastal to deeper waters, which could be due to a nutrient decrease in the Rhone (Feuilloley et al., 2020). Feuilloley et al. (2020) have also shown that environmental conditions have globally changed in the Gulf of Lion, with a major change in the mid-2000s, affecting the upwelling and frontal activities, the Rhone River discharge, the deep-water convection, the concentration of chlorophyll-a, which became lower and the Sea Surface Temperature (SST) which increased. Those changes could have caused a decrease in the plankton production and consequently impacted the small pelagic fish community that showed similar patterns of variations as environmental conditions.

As previously mentioned, plankton data from DCF surveys have not been exploited so far in the frame of the MSFD. Given the amount of data available for PELMED and the amount of time for the internship, we chose to focus on zooplankton and to carry out the first numerical exploratory analyses on this plankton compartment as it constitutes an intermediate and key component of the pelagic food web, zooplankton controlling phytoplankton dynamics and being themselves under the top-down control of zooplanktivorous predators. PELMED surveys offer the opportunity to target a seasonal period (summer spawning) and site (GoL) of interest regarding small pelagic fish dynamics namely Sardines (*Sardina pilchardus*) and anchovies (*Engraulis encrasicolus*; Regimbart et al., 2018). Therefore, given the strong trophic link between zooplankton and fish, a better understanding of zooplankton composition, distribution pattern, and variability would allow to integrate these biotic components in the assessment of pelagic fish distribution.

The main goal of this internship was to study the distribution patterns of summer zooplankton communities over a 7 year period (2013-2019) in the gulf of Lion. More precisely, we firstly aimed to identify major functional and taxonomic zooplankton groups in the Gulf of Lion during the summer period, to define their variability in space and at interannual scale. Secondly, we aimed to study how zooplankton communities and particularly copepods, responded to environmental changes i.e. we wanted to point out which functional or taxonomic group was more sensitive to changes in environmental conditions and which environmental forcing was responsible for observed changes. Identifying a pattern or a more sensitive functional group to environmental conditions could be useful to identify areas of interest, groups of interest to monitor and then to be targeted into the PelHab monitoring programme. This latter part of the internship is discussed as monitoring perspectives in the manuscript.

2- MATERIALS AND METHODS

2.1. Data collection

2.1.1 - PELMED sampling design

Hydrological and zooplankton data were collected during PELMED surveys from 2013 to 2019.

PELMED is an acoustic and trawl identification survey which covers the Gulf of Lion and the Provence Alpes Côte d'Azur (PACA) region. This survey generally occurs at the end of June and during the month of July. The main goal of PELMED is to provide fishery-independent data for the purposes of stock assessment of small pelagic fishes (Bourdeix, 1985). Since 2015, PELMED has been adapted and optimized regarding data collection and sampling to suit the needs of Marine Strategy Framework

Directive (MSFD) descriptors (e.g. Pelagic habitats, eutrophication, marine mammals, birds, marine litter; (Baudrier et al., 2018). In answering this goal of optimisation, PELMED allows an integrative sampling of the pelagic ecosystem from planktonic organisms to marine mammals as well as sampling of environmental conditions (i.e. hydrology and physico-chemistry). PELMED sampling design follows 9 parallel transects separated by 12 nautical miles, each being perpendicular to the coast (Figure 1). Samples are collected at the end of each transects or after each trawl.

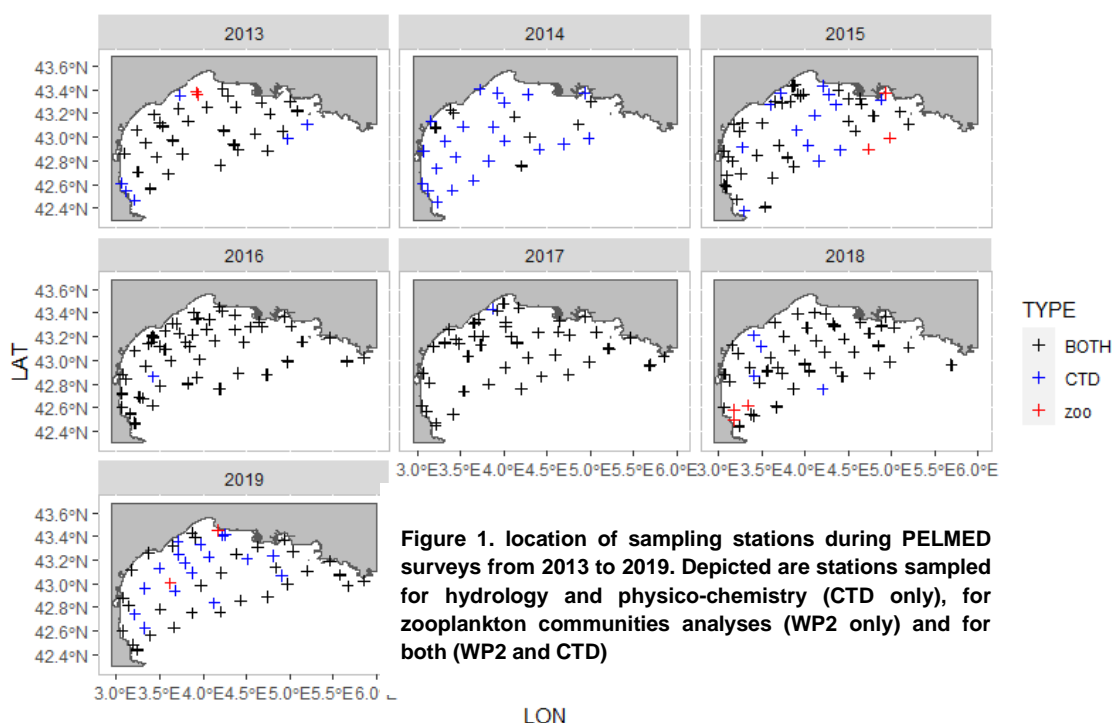


Figure 1. location of sampling stations during PELMED surveys from 2013 to 2019. Depicted are stations sampled for hydrology and physico-chemistry (CTD only), for zooplankton communities analyses (WP2 only) and for both (WP2 and CTD)

The stations where hydrological and zooplankton data were collected, were not always located at the same site (except for the stations located in the edges of each transect) given that trawl haul stations depend on acoustic detection of fish shoals (Figure 1). Number of stations sampled also varied from one year to another (Table 1). Note that in 2014, few stations were sampled for both WP2 and CTD, only 7 for WP2 i.e. zooplankton samples. At each station, vertical profiles of hydrobiological parameters (temperature, salinity, fluorescence, photosynthetically active radiation, oxygen, turbidity, and pH) were obtained using a CTD SBE19 Plus. The CTD is mounted on a “rosette” carrying 6 Niskin bottles for seawater sample collection. Zooplankton was sampled using a WP2 net (see section 2.1.3.).

Table I: Number of CTD casts and zooplankton samples collected (WP2 net) each year during PELMED surveys

Year	2013	2014	2015	2016	2017	2018	2019
Number of CTD casts	45	30	52	59	46	52	52
Number of zooplankton samples	32	7	37	54	44	48	31

2.1.2 - Environmental data

Environmental data originated from two sources. Firstly, the PELMED *in situ* dataset provided hydrological and physico-chemical parameters collected at the same time as zooplankton communities (see section 2.1.1.). Secondly, satellite derived products for sea surface temperature,

wind (intensity and direction), suspended matter and phytoplankton biomass (chlorophyll-a) were used to complete the spatial coverage of *in situ* data and to have a synoptic snapshot of the entire Gulf dynamics in July. The spatial gradient of temperature could be blurred by using *in situ* surface temperature data from a specific survey, and thus misleading when discriminating the existing spatial pattern (Huret et al., 2018). However, the two temperature datasets (*in situ* and satellite derived products) were kept because they are complementary.

2.1.2.1-*In situ* data from PELMED surveys

a- Temperature and salinity

Bottom and sea surface temperature data (°C) were obtained from CTD profiles at each sampling station and were coded (BotTemp) and (SurfTemp), respectively. The same holds for salinity regarding surface (SurfSal) and bottom (BotSal) values.

b- Water column characteristics

Additional variables were computed from CTD profiles to provide further information into water column characteristics (e.g. stratification, mixed layer depth, intensity of vertical mixing and river plume indice).

The potential energy deficit (defEpot) was computed following Huret et al., (2013; Eq. 1). It corresponds to the energy required to homogenize the density of the water column. In other words, the deficit of potential energy characterizes the water column stratification:

$$Def.pot = \frac{1}{H+\xi} \int_{-H}^{\xi} (\underline{p} - p_z) g z dz \quad (eq.1)$$

where \underline{p} is the mean density over the water column (obtained from CTD profiles), p_z the density at depth z , H the bathymetry and ξ the height of free surface. The greater the deficit, the stronger the stratification.

The equivalent water height (Heq) is a river plume index that highlights vertical mixing. It can be defined, following Choi and Wilkin (2007; Equation 2) , as:

$$\delta_{fw} = \int_{-H}^{\xi} \frac{S_0 - S_z}{S_0} dz \quad (eq.2)$$

where S_0 is a reference salinity of 38. S_z is the salinity at depth z and dz is the depth difference. High Heq values correspond to an important vertical mixing.

The mixed layer refers to the surface layer where physical parameters such as salinity, temperature and density are almost homogeneous. The mixed layer maximum depth (ProfHmel) was calculated as the maximum depth where the potential density is not homogenous anymore. It is preferable to use potential density or sigma t (σ_t) as estimators for ProfHmel, primarily because it is the density structure that directly affects the stability and degree of turbulent mixing in the water column. The ProfHmel was computed using an integral depth-scale method also called the trapping depth by Price

et al., (1986) where, z_a and z_b are respectively a near-surface depth and an arbitrary reference depth (100 m) and $\sigma_{\theta_b} = \sigma_{\theta}(z_b)$ et $\sigma_{\theta_a} = \sigma_{\theta}(z_a)$

2.1.2.2- Satellite data

a - Sea Surface Temperature (SST)

The satellites have been used in addition to CTD data because the surface temperature data from PELMED were not collected at the same time. Some stations were sampled at the end of June and others at the end of July. This one month of difference in sampling time can blur the distribution patterns. As a complementary dataset, Satellite SST data were obtained from the Copernicus Marine Environment Monitoring Service (CMEMS) platform³ to allow a more regular spatial coverage of the whole sampled area. All data were optimally interpolated (level-4, L4) on a 0.05° resolution grid using the level-3 climate data record provided by the ESA CCI and the Copernicus Climate Change Service, and an adjusted version of the Advanced Very High-Resolution Radiometer (AVHRR) Pathfinder dataset version 5.3 to increase the input observation coverage (CMEMS Product description). Data provided daily, based on satellite estimations, and covering a 38 year-period (from 1982 to 2019) were averaged for July month each year.

b- Chlorophyll a (satellite derived products)

Monthly averaged (from daily images) chlorophyll-a (Chl-a) concentrations for the month of July were derived from the MODIS/AQUA remote-sensing reflectance, processed by the coastal OC5 algorithm with updated Look-Up-Tables (Gohin et al., 2020). Chl-a concentration is expressed in mg m^{-3} .

c- Turbidity and non algal part of suspended matter (satellite derived products: MODIS)

In order to characterise water masses transparency, satellite derived products were obtained at 1 km resolution using the OC5 algorithm of Gohin et al.,(2002) applied to MODIS (Moderate Resolution Imaging Spectroradiometer) marine reflectance. Only the non-algal part of the total suspended matter (TSM) was considered here. In order to estimate TSM, a semi-analytical algorithm (Gohin et al., 2005) was used. In this semi-analytical method, absorption and backscattering by phytoplankton are derived from preliminary estimations of Chl-a concentration by OC5. The radiance at 550 nm and 670 nm are used to estimate the non-algal suspended particulate matter (SPM). Depending whether the non-algal SPM concentration obtained is less or more than 4 g.m^{-3} , then the non-algal SPM derived from the 550 nm or 670 nm radiance is used, respectively (Gohin et al., 2020). The turbidity is estimated from SPM following equation (3):

$$\text{Turbidity} = 0.54 \text{ TSM} \quad (\text{eq. 3})$$

Daily data were averaged (arithmetic mean) over the month of July to cover PELMED survey period.

d- Hydroclimatic forcing: wind intensity and direction

Wind data were obtained from the CMEMS. Wind characteristics were calculated from ASCAT-A and ASCAT-B scatterometer retrievals and comprised monthly averaged wind speed (m s^{-1}), zonal and

³ <https://resources.marine.copernicus.eu/>

meridional wind components (m s^{-1}), wind stress amplitude (Pa) and the associated components (zonal and meridional). They are calculated as arithmetic means of ASCAT daily wind analyses. Monthly wind speeds of June and July were estimated and mapped on a 0.25° resolution grid.

Available satellite data were imported from several sources on a different grid resolution and spatial extent. Using the R package 'raster', satellite data have been re-projected onto a common grid with a mesh size of 0.1° (~ 10 km) for both latitude, and longitude, resulting in 390 cells (see section 2.3.2 for details on the choice of this grid resolution).

2.1.3- Zooplankton data

Zooplankton was sampled using a WP2 (200 μm mesh sieve, 0.25 m^2 diameter) plankton net equipped with a flowmeter and fitted with a filtering cod-end (2 L). At each station, vertical hauls were performed through the upper 100 m of the water column (1 m s^{-1} ; 20 min duration). Onboard samples were sieved on 100 μm mesh and preserved in buffered formalin (4% final concentration).

At the laboratory, samples were counted and identified down to the species level by Dr. Antoine Nowaczyk (UMR EPOC, Station Marine d'Arcachon). Under a fume hood, the sample was firstly sieved (200 microns) and rinsed thoroughly with water to remove any remaining traces of formalin. Then, the entire content was introduced in a measuring cylinder (100 or 250 mL) and filled with water until reaching the chosen volume. This volume depends on the quantity of organisms in the sample. A parafilm blocks the opening and the content was homogenized through back-and-forth movements. An aliquot (a small part) was quickly taken with a micropipet (1 or 5 mL) and then dropped in a Dollfus tank. Counting of sub samples was carried out by stereomicroscopy (NIKON SMZ25). The smallest fraction for PELMED sample count consisted of in $1/250$, i.e. 1 mL for a 250 mL sample. If a taxon abundance was too low, then other sub-samples were counted. Taxonomic analyses were carried out until the entire sample was counted regarding the rarest taxa. In other words, concerning dominant taxa, at least 30 individuals were counted and the minimal number of identified individuals in a given sample was 400 (for all taxa). Finally, after each count, all individuals were sieved, concentrated once again into the original vial and preserved with the original 4% formaldehyde/water solution.

2.2- Building a zooplankton functional traits database

The first working step consisted in the construction of a zooplankton database including information about year, abundance, taxonomy, latitude, longitude, and functional traits. Several steps were needed to achieve this goal: (i) data homogenization between years, (ii) data selection based on taxonomic information and finally (iii) adding functional traits information to the standardized database. All the table transformations and data analyses were carried out using R (R Core Team 2020; version 4.0.3).

2.2.1- Harmonization/homogenization of available data

PELMED data from 2013 to 2018 were imported from the Quadrige² database (Figure 3: table D2). As 2019 data were not yet archived, raw data were available in a different data format than the Quadrige² database (Figure 3: table A, table B). The first step consisted in reorganizing the raw dataset, adding spatial information (table B), metadata and homogenizing taxa names between 2019 and other years (Figure 3: table C). Taxonomic data were in fact heterogeneous as several levels

were considered (e.g., class, order, family, genus, and species) and some labels needed to be verified (Figure 3: table C). This taxonomic heterogeneity could be an issue for future data analyses. Thus, in order to better discriminate taxonomic levels and identify taxa, the apicalID from WORMS⁴ was added to each observation (Figure 3: table E).

2.2.2- Data selection

The target group of the study were copepods since they constitute the most abundant group of zooplankton, representing 42 to 66% of the total abundance during PELMED surveys (Figure 2). Within the copepods, only data of adult stages were kept because adults have the steadiest functional traits. Indeed, depending on development stages, sizes, trophic regimes and DVM behaviors could differ (Pomerleau et al., 2015). Meroplankton was not considered because it was not the focus of this study and represented less than 11% of total zooplankton abundance (Figure 2).

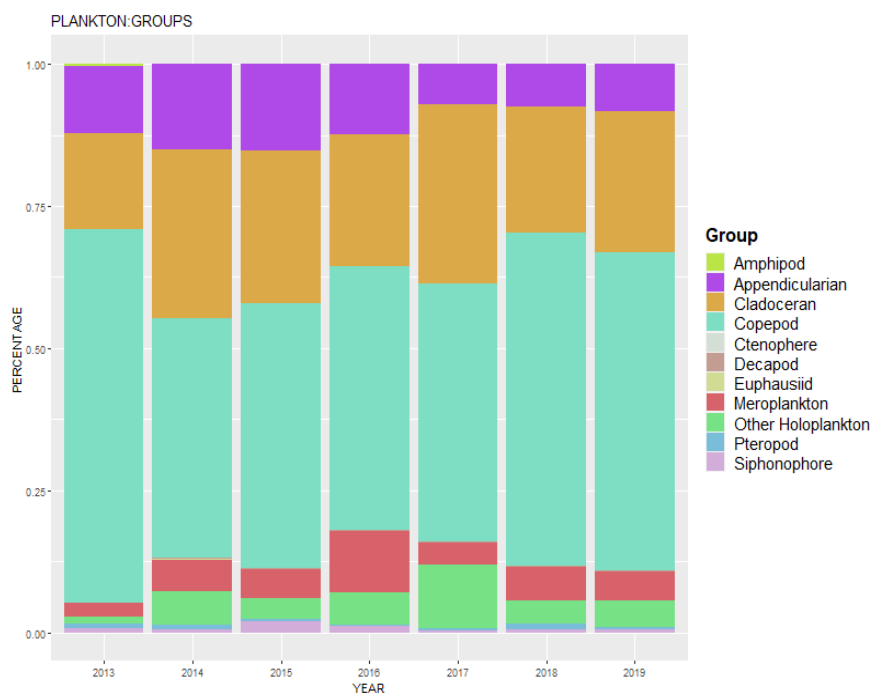


Figure 2: Relative abundance of dominant plankton groups from 2013-2019 during PELMED surveys. Depicted are main holoplankton groups and total meroplankton.

2.2.3- Zooplankton functional traits

Functional traits are defined as any morphological, physiological or phenological feature measurable which impacts fitness indirectly via its effects on growth, reproduction and survival (Violle et al., 2007). Traits were chosen following already published studies on copepods functional ecology (Benedetti et al., 2016; Brun et al., 2016; see Table II). They comprised minimal length, maximal length, trophic regime, feeding strategy, spawning strategy, DVM behaviour (diel vertical migration) and pelagic layer occupied. The main identified traits were collected from Benedetti et al.,(2016) and Brun et al., (2016).

⁴ World Register of Marine Species

Table II. Functional traits derived from Benedetti et al. (2016)* and Brun et al. (2016).** The number of copepod species concerned by each trait for PELMED surveys is indicated

FUNCTIONAL TRAITS	MODALITIES	NUMBER SPECIES	EXPLANATION
Minimal Length	Continue value (mm)	44	Min body (cephalothorax) length of adults*: 0,3 to 3,2 mm
Maximal Length	Continue value (mm)	44	Max body (cephalothorax) length of adults*: 0,86 to 8,5 mm
Trophic Regime	Herbivore	1	Only herbivore.
	Carnivore	6	Only carnivore.
	Omnivore	17	Omnivore without preferences.
	Omnivore-carnivore	2	Omnivore species but with carnivore preferences.
	Omnivore-herbivore	15	Omnivore species but with herbivore preferences.
	Omnivore-detritivore	3	Omnivore species but with detritivore preferences.
Feeding Strategy	Active ambush	8	Organisms ambush their prey (sit and wait strategy) **
	Cruising	5	Organisms cruise through the water in search of prey**
	Filter	20	Organisms produce a feeding current to feed**
	Mixed	11	for species that can switch between the 3 strategies*
Spawning Strategy	Sac-spawner	12	eggs are carried by the females within sacs prior to hatching*
	Broadcaster	32	females release the eggs directly in the water*
	No	16	Non-migrant *
Diel vertical migration (DVM) behaviour	Weak	24	DVM occurs within tens of metres*
	Strong	3	over several hundreds of metres*
	Reverse	1	for species that migrate deeper at night*
Pelagic Layer	Epipelagic	23	preferential habitat layer: 0-200 m*
	Epimesopelagic	13	preferential habitat layer: 0-1000 m*
	Epibathypelagic	8	preferential habitat layer: 0-4000 m*

Although a strong literature review was carried out, some traits information was still missing. In this case and if the species did not belong to the 99% most abundant copepod species inhabiting the Gulf of Lion from 2013-2019, they were removed from the analyses. This was the case for *Pontella lobiancoi*, *Pteriacartia josephinae* and *Pontella mediterranea*, representing respectively 0.004%, 0.001% and 0.010% of the total copepod abundance. In the second case, the missing trait information for a given species was completed using the trait defined at the genus level otherwise using the trait clustering of (Benedetti et al., 2018). This approach was based on two assumptions: “two species of the same genus share the same functional trait” and “two species in the same functional group (Benedetti et al. 2018) share the same trait”. The cluster-based method of Benedetti et al. (2018) was used for 4 species. *Diaxis pygmea* (trophic regime and feeding strategy), *Haloptilus longicornis* (reproduction strategy), *Haloptilus mucronatus* (reproduction strategy) and *Isias clavipes* (reproduction strategy). For *Oithona similis* and *Lucicutia ovalis*, DVM behaviour was completed using the traits reported at the genus level.

The final matrix of copepod abundance comprised 7 functional traits, 43 species, 7 years and 253 sites.

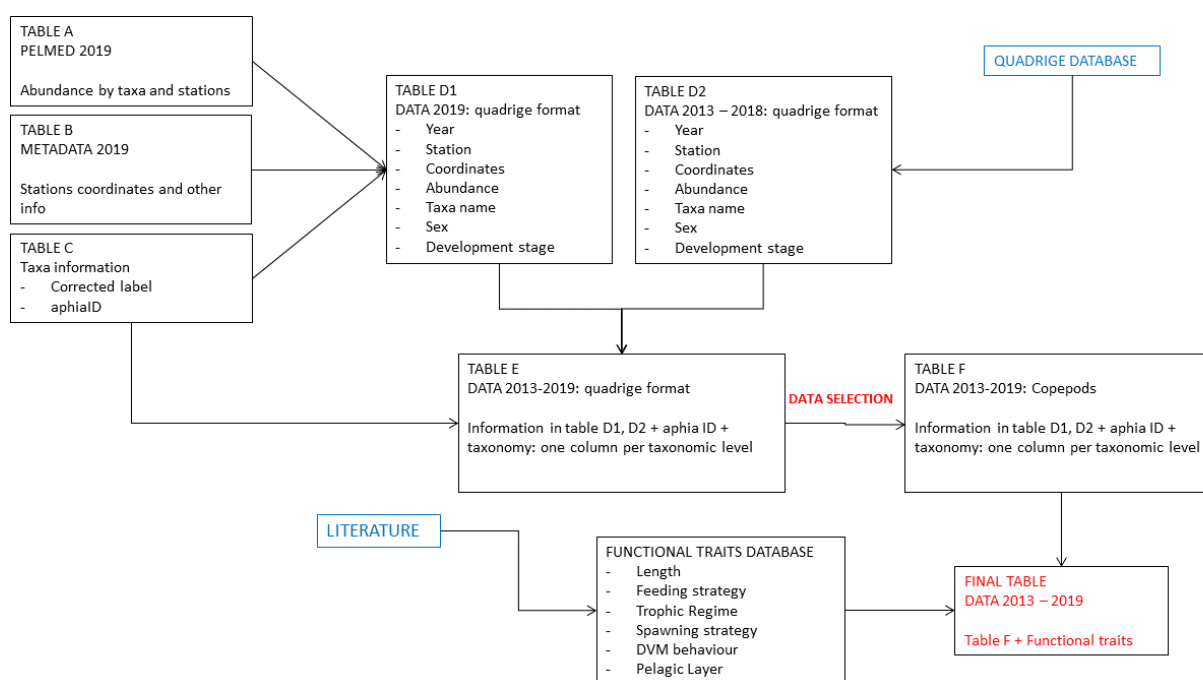


Figure 3: Steps of the database construction for copepod functional traits.

2.3- Data analyses

2.3.1- Exploratory analyses

Raw data were first analyzed regarding structure and interannual variability of holoplankton, meroplankton, total zooplankton abundance and finally, copepod species abundance. In order to limit the number of species to be mapped and represented in the different graphs (maps and bar plots of

relative abundance), cumulative percentages of abundance were computed and allowed to consider only species representing 99% of total abundance over the study period (2013-2019).

All graphs and maps were made with the 'ggplot2' R package.

2.3.2- Mapping *in situ* and satellite derived data

The challenge here was to find a suitable mapping method for all the available datasets. Indeed, the heterogeneity of the survey sampling design and the wide area covered complicated the spatial interpolation (*i.e.* environmental variables and zooplankton abundance). In order to identify the most suitable spatial interpolation technique several methods were compared and tested on the zooplankton dataset (Appendix 1). Before spatial interpolations, zooplankton abundances were log transformed ($\log X+1$) to normalize the dataset and minimize the effect of extreme values and the skewness of the original data.

Then, ordinary kriging has been tested using the R 'Geostats' package. Ordinary kriging is the most used geostatistical method. It serves to estimate a point or a block value, for which a variogram is known, using data in the neighborhood of the estimation location (Wackernagel, 1995). This method was sensitive to the sampling design (*i.e.* especially the uneven sample size for each distance lag), as many of the variograms poorly behaved, and they did not rise smoothly to a sill, and they jumped around erratically, or even decreased with distance. Besides, because of the irregular sampling design between years (*i.e.* the geographical positions of the hydrological stations change from one year to another, see Figure 1), the mean variograms method (*i.e.* averaging several annual variograms as a way to improve the spatial model) could not be used.

Another method was tested. An automatic procedure was set up for each species at a given year, which chose the best method between Thin Plate Spline (TPS), Inverse Distance Weighted (IDW), ordinary kriging and nearest neighbourhood interpolation based on a cross validation procedure (*i.e.* 3-fold cross validation) and the calculation of root-mean-square error (RMSE) as a validation/comparison criterion. RMSE measures differences between observed and predicted values and was used to select the best method at each step. The TPS method (Duchon, 1976) is a spline-based technique for data interpolation and smoothing which fits a thin plate spline surface to irregularly spaced data. Smoothing parameter is chosen by generalized cross-validation. The IDW (Shepard, 1968) calculates estimation values in each cell of the grid by averaging the values of the data points located in the neighbourhood of the cell. Points which are closer to the centre of the estimated cell have more weight in the averaging process. Weights are proportional to the inverse of the distance between the data point and the estimation location, then raised to the power value p . The parameter p is determined automatically by means of a cross validation. The nearest neighbourhood method is applied when $p=1$. Then a value is assigned to a certain grid cell from the nearest observation. This automatic procedure has the advantages of (i) not necessarily requiring variograms which may be influenced by the sample design and (ii) by comparing four different methods, it increases the likelihood of selecting the most appropriate method for the considered dataset. However, the drawback of this approach is that since different interpolation methods are selected depending on years and species, this results in maps displaying a high degree of heterogeneity in terms of spatial patterns and does not seem very comparable.

After multiple testing, block averaging (Petitgas et al., 2009; Petitgas et al., 2014) appeared to be the best suited method for mapping our copepod dataset. It is considered as a simple procedure which produces gridded maps from the observation, *i.e.* data are averaged by block over a grid. Block averaging is already used to provide a time series of an annual survey map from data collected during the PELGAS survey in the Bay of Biscay and which have a sampling design identical to the PELMED survey (Doray et al., 2018a; Doray et al., 2018b). In order to produce maps from the data, this method requires to set a grid and a smoothing parameter u , here the value used for the whole dataset is the same as PELGAS, *i.e.*, $u=2$.

Grid size can be optimized by setting a minimum number of sample points averaged in each map cell, and trying out various grid sizes until meeting this criterion. The grid mesh size was set to 0.1° (~ 10 km) for both latitude, and longitude, resulting in 390 cells. This resolution was chosen as it cannot be too small given the large size of the area to be mapped (from 2.89°W to 5.5°W and from 42.2°N to 43.7°N) and the scarcity of data for specific years (e.g. 2014). In fact, if the grid mesh is too small, it will lead to observing a large number of cells with no data. On the contrary, if the grid mesh is too high, the map will not contain enough cells to accurately and clearly visualize data distribution patterns. The block averaging is influenced by the grid origin position. In order to decrease this bias, the origin of the grid is drawn randomly in a larger block that comprises four smaller blocks (*i.e.* smoothing parameter u), as shown in Figure 4 (Masse et al., 2018). This will reduce the dependence of the averaging from the grid origin and a local smoothing will occur. Once the origin of the grid is settled, data are averaged for each grid cell N times (here $N=200$). Then, in each cell the 200 values (mean and standard deviation) obtained are computed. In summary, the procedure applied is the following: (i) 200 grids are generated, each with a different origin; (ii) block averaging is performed for each; (iii) all grids are then superposed; and (iv) the mean in each cell is calculated by averaging the cell means of all grids (Doray et al. 2018a, (Lavorel et al., 2008)2018b).

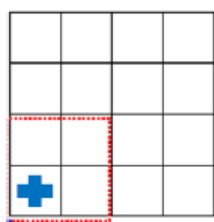


Figure 4. Illustration of the block averaging method principle as described in Masse et al. (2018). Schematic of the standard grid (black: $0.25 \times 0.25^\circ$), the large block (dashed red line) in which the grid origin is randomized. The cross (blue) shows the position where the origin of the grid is positioned to present the results .

Despite block averaging, certain cells of the grid presented missing values. In this case, ordinary kriging was used to interpolate values in the corresponding cells.

At the end, one map per species or per environmental variable was generated for each year for the 2013 -2019 period. The block averaging procedure was implemented using the 'Echo' R package.

2.3.3- Functional traits: community weighted mean

In order to produce maps reflecting the functional composition of copepod communities, in terms of length, trophic regime, feeding strategy, spawning strategy, DVM behaviour and pelagic layer, we measured the community-level weighted means of trait values (CWM; e.g. Lavorel et al., 2008). The rasters of abundance previously generated by block averaging were used to map the functional traits.

The function *functcomp* from the package FD was used to return community-weighted means (CWM) of trait values in each cell. For a continuous trait, CWM is the mean trait value of all species present in the community, weighted by their relative abundances. For a discrete trait, the abundance of each individual class is computed.

2.3.4- Ecological and environmental indicators

2.3.4.1 Environmental turnover

In order to summarize the environmental variability that has occurred in the Gulf of Lion and in a multivariate manner, we calculated a pairwise Euclidean distances matrix after centering and scaling environmental variable maps resulting from the block averaging interpolation. A PCoA was then performed on the distance matrix. The results of the PCoA were mapped on the same grid as the block averaging and a RGB gradient was set up depending on the position of cells on the two PCoA axes. To create the RGB gradient, the values of both axes were first scaled between 0 and 1 and then the function *rgb* from the *grDevices* package was applied. Values on axis 1 give red intensity values, values on axis 2 give green intensity values and blue intensity values are given by (1-values) on axis 1. The resulting maps reflect the degree of environmental dissimilarity between each pair of pixels. The more the colors are different and the more the environmental differences are important.

As PCoA is a visualization technique and is not a statistical assessment of sample separation or correlation, we then calculated multiple regression of environmental variables with ordination axes (environmental variable is used as dependent and the two first PCoA axes as explanatory variables) using the *envfit* function. The projections of points onto vectors have maximum correlation with corresponding environmental variables. This is equal to fitting a linear trend surface (plane in 2D for a variable); this trend surface can be presented by showing its gradient (direction of steepest increase) using an arrow.

2.3.4.2- Spatial and temporal variability of the alpha taxonomic diversity

Alpha diversity describes the species diversity in a community at a local scale. In order to measure the alpha taxonomic diversity, four ecological indices were computed, using the *vegan* package: Shannon, Simpson, Pielou and the specific richness. These indices were mapped on the same grid used for abundance and environmental parameters. These indices were chosen because they are among the mostly used and they are easily interpretable (Richirt et al., 2019). They measure different parameters as the number of species (e.g specific richness), the species evenness (e.g Pielou) or they combine both (e.g Shannon and Simpson).

The Simpson index (Simpson, 1949) is defined by the probability for two random individuals to be in the same species. It can be written as the following equation (eq.4): $L = 1 - \sum(p_i^2)$, with $p_i = n_i/n$, n_i is the number of individuals in the species i and n is the total number of individuals.

The Shannon index (Shannon, 1948) is defined by $H = -\sum(p_i * \log_b(p_i))$ (eq.5), with $p_i = n_i/n$, n_i is the number of individuals in the species i , n is the total number of individuals and b is the logarithm base. This index increases when the specific richness and the equitability of the community increase.

Pielou index (Pielou, 1966) is calculated as : $J = \frac{H}{\log_2(S)}$ (eq. 6) ,with H as the Shannon index and S as the specific richness. It represents the species' evenness. It expresses the degree of species equality in the sample. This index informs if there are dominant species in the community and varies between 0 (one dominant species) and 1 (equal distribution of species).

The specific richness is the total number of species.

2.3.4.3- Beta functional diversity

In this part, we were interested in studying the relationship between functional traits and environmental variables. Kleyer et al (2012) reviewed several multivariate methods in order to assess species and community functional responses to environmental gradients. In this study, only the redundancy analysis (RDA) and the RLQ were used as both methods were the most suited to provide answers to our questions: whether and how did average trait expressions of copepod communities change along environmental gradients? Both analyses are based on at least one of these three tables: a sites-by-species table (L), a sites-by-environmental variables table (R) and a species-by-traits table (Q). The site-by-species data were log-transformed as well as chl-a, turbidity and suspended matter data whereas environmental data were centred-scaled .First, a correspondence analysis was performed on the L table in order to obtain the weight used in the analysis of Q and R. The functions *dudi.coa* (on L table), *dudi.pca* (on R table) and *dudi.hillsmith* (on Q table) from the package *ade4* (R version 4.0.2) were used. Then a RLQ analysis was carried out on the results of these three analyses.

RLQ is a three table (R,L and Q) method (Dolédec et al., 1996). It analyses simultaneously the three tables in order to summarize and represent the main patterns of covariation between traits data and environmental variables. In other words, the aim here was to find the linear combination of environmental variables and the linear combination of traits data that maximized the coinertia criterion. This criterion is the product of the environmental variance, the species variance and the squared cross-correlation between environment variables and traits mediated by L table (Kleyer et al. 2012). The RLQ uses the *rlq* function from the *ade4* package.

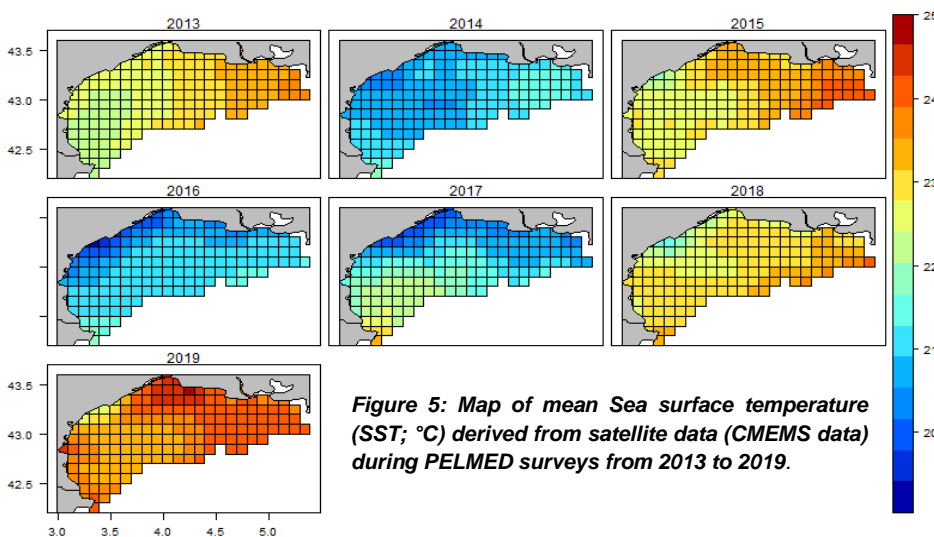
An RDA (Rao 1964) was performed using the function *pcaiv* from the package *ade4*. RDA is an extension of principal component analysis (PCA) but axes are constrained to be linear combinations of explanatory variables. As in PCA, RDA identifies orthogonal axes that maximally explain variation in species composition, or in trait composition (Palmer et al., 2008; Legendre and Legendre, 2012). One response matrix, the weighted-traits matrix, was analyzed with regard to a corresponding explanatory matrix, i.e. R, the environmental variables matrix (Legendre and Anderson, 1999). To sum up, as a community based approach, the RDA allows the assessment of functional traits response to environmental variables (Nygaard and Ejr nes, 2004; Kleyer et al., 2012). It was performed on the community weighted mean of traits matrix, generated in section 2.3.3. RDA results⁵ were then mapped on the same grid as previously and a RGB gradient was set up depending on the position of cells on the two RDA axes.

⁵ RLQ results were similar to RDA results. RLQ was very sensitive to functional traits which were under-represented (reverse DVM, herbivore). Only the RDA results will be presented because they appeared to best discriminate our observations.

3- RESULTS

3.1- Interannual and spatial variability of environmental conditions

Over the period 2013-2019, SST satellite observations ranged between 19.40°C and 24.64°C (figure 5). Four warmer years could clearly be identified (2013, 2015, 2018 and 2019) with seawater temperature reaching values up to 24.64°C, particularly in 2019, and not going below 21.35°C. The mean SST for these warmer years was 23.09 ± 0.57 °C. During these warmer years, temperature distribution followed a eastern-western gradient with lower values in the western part and higher values in the eastern part. On the contrary, during July 2014, 2016, and 2017 lower temperatures were recorded, with the lowest values being 19.40°C and the temperature did not exceed 23.35°C. The mean SST for these years was 21.01 ± 0.56 °C. During these slightly 'colder' years, mean July temperature followed a more North-South (i.e., inshore-offshore) distribution pattern, with lower values recorded along the coasts.



Over the period 2013-2019, surface salinity values ranged between 36.30 and 38.21. Years can be separated into several groups according to spatial distribution of salinity (Figure 6). Four years, 2013, 2014, 2015 and 2019, were characterized by lower salinity values down to 36.30 near the coast. Especially in 2013, 2014 lower salinity values were recorded near the Rhone and its dilution plume. In 2015 and 2019, coastal lower salinity waters were also observed but the general distribution pattern highlighted a wider distribution of lower values in the west, resulting in a pronounced western-eastern gradient. Years 2016 and 2018 shared a similar distribution pattern with a small area of lower salinity offshore between 36.76 and 38.17, and particularly higher values in the eastern part of the sampled area. The year 2017 was rather a homogenous year regarding surface salinity distribution. This was in fact the year presenting the smaller variability in salinity with values ranging between 37.68 and 38.21.

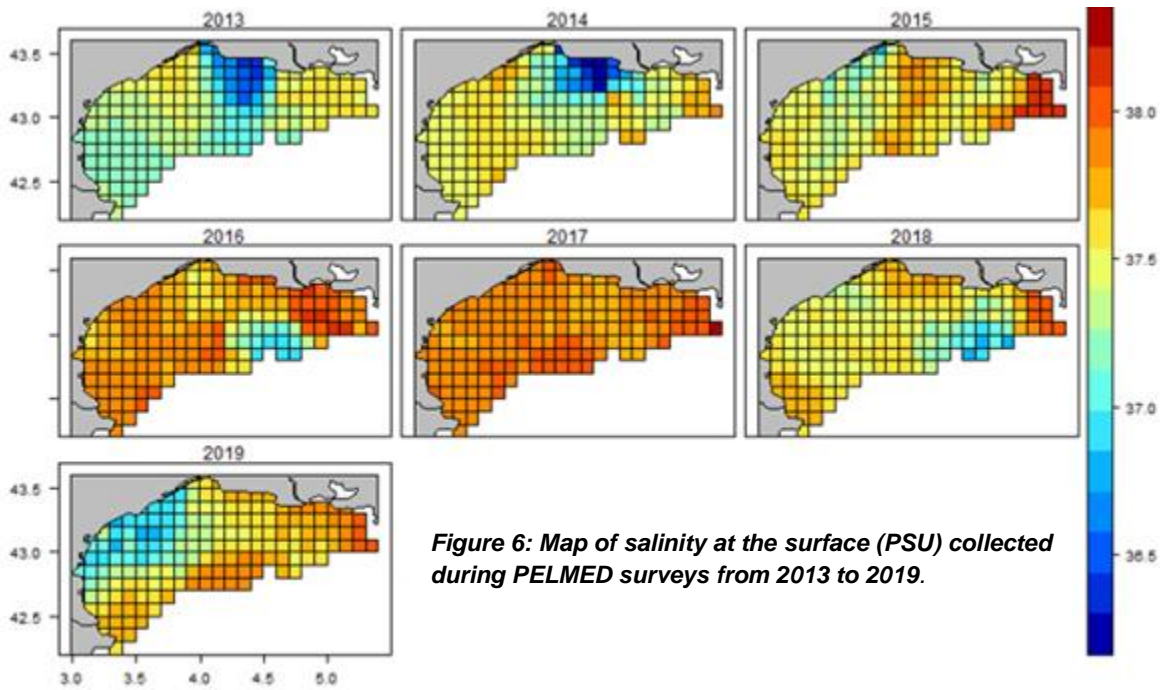


Figure 6: Map of salinity at the surface (PSU) collected during PELMED surveys from 2013 to 2019.

The northwestern direction of the wind prevailed in July over the study period 2013-2019. The wind speed however exhibited a higher variability between years (figure 7 and appendix 2). In 2013, wind intensity was rather low compared to other years, with values between 0.29 m s^{-1} and 1.47 m s^{-1} . 2014 and 2016 were the years exhibiting the strongest winds with mean wind speeds of $4.23 \pm 0.34 \text{ m s}^{-1}$ and $3.49 \pm 0.44 \text{ m s}^{-1}$, respectively. Besides, the highest wind speed value of 5.02 m s^{-1} was reached in July 2014. For the remaining years (2015, 2017, 2018 and 2019) the wind speed showed little variation and mean values ranged between $2.38 \pm 0.36 \text{ m s}^{-1}$ and $2.78 \pm 0.25 \text{ m s}^{-1}$.

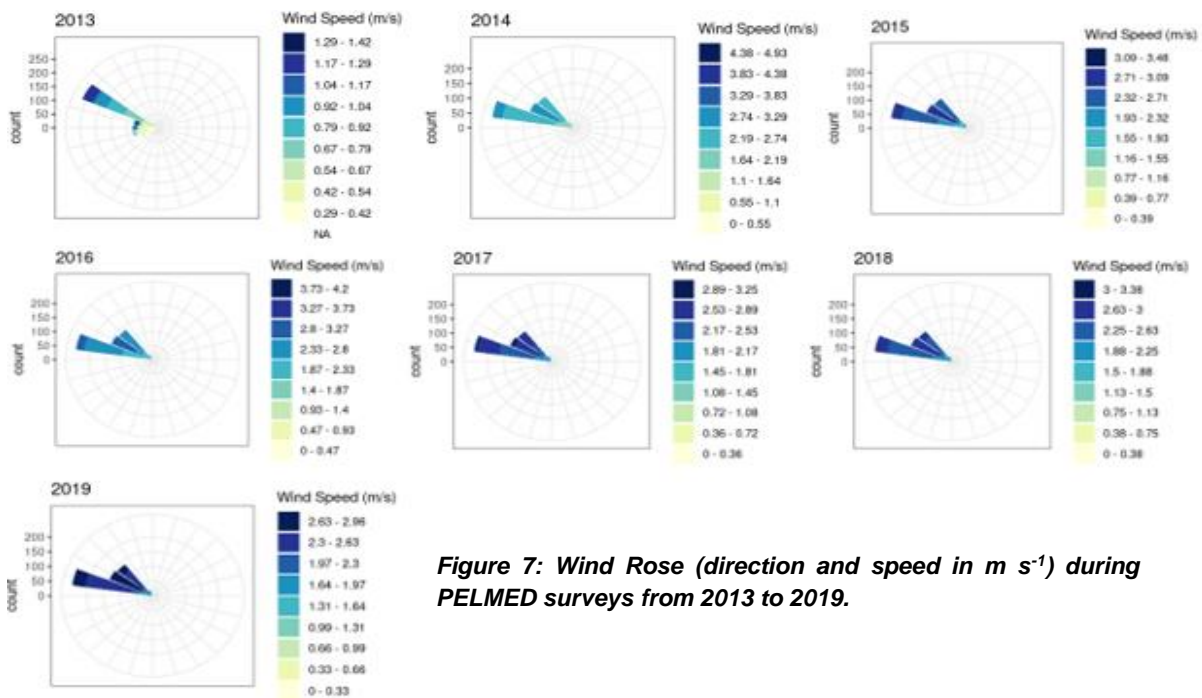
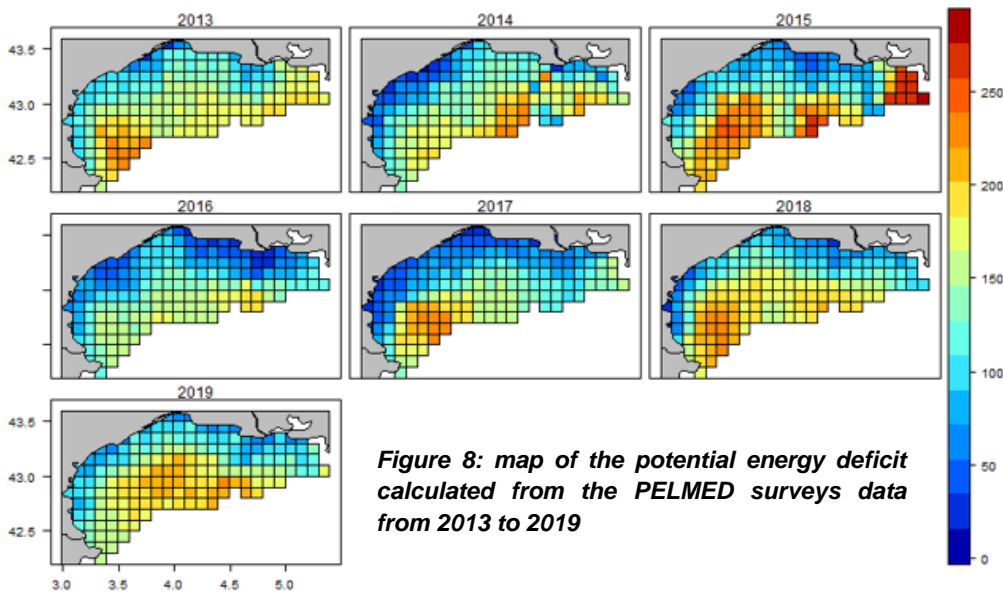
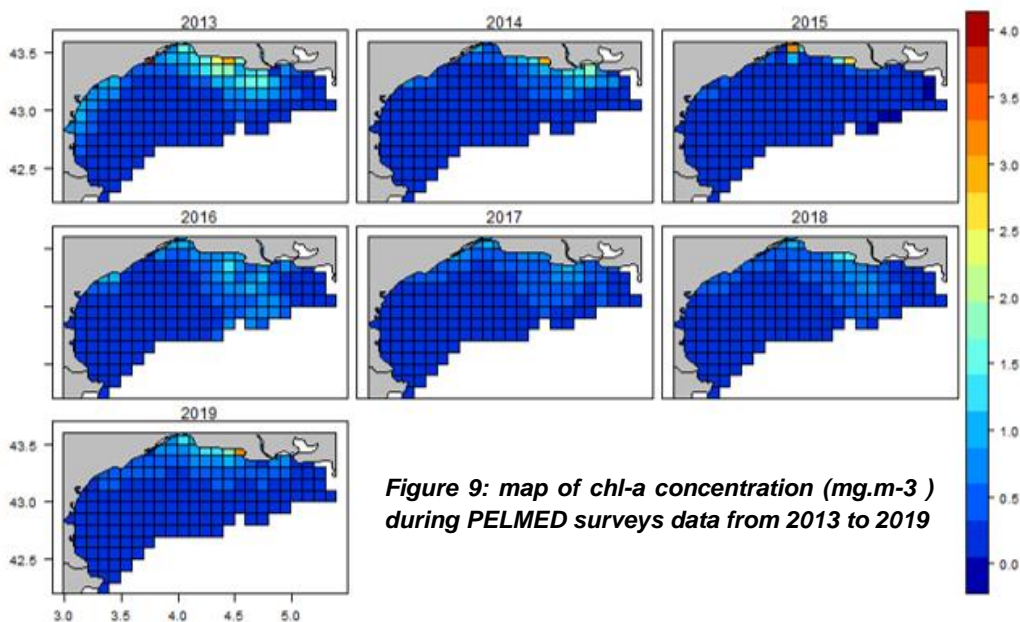


Figure 7: Wind Rose (direction and speed in m s^{-1}) during PELMED surveys from 2013 to 2019.

Regarding the deficit of potential energy (DefEpot), all the years presented the same distribution pattern with an increasing gradient from the coast to offshore area (Figure 8). In other words, the water column in July was always less stratified and more mixed near the coast, contrarily to offshore areas where the stratification was stronger.



The distribution pattern of chl-a concentrations was rather similar from one year to the other (Figure 9)⁶. Concentrations were always higher near the coast, in the more mixed area, reaching values up to 3.25 mg m⁻³. Offshore, in the stratified area, minimum values were 23 times lower (0.14 mg m⁻³) and never exceeded 1.79 mg m⁻³. Mean values were the highest in 2013 (0.71 ± 0.60 mg m⁻³) whereas lowest mean values reaching 0.39 ± 0.25 mg m⁻³ were recorded in 2017.



⁶ The turbidity followed the same pattern as the chl-a. In order to avoid repetition the figure is in appendix 3.

The two first axes of the PCoA represented 52.1% of the variability of environmental data (31.7% for axis 1 and 20.4% for axis 2). All the environmental variables were significantly correlated to the two first axes of the PCoA (results from the *envfit* analysis ; p value ≤ 0.001 for each variable considered). Two groups of years presenting similar environmental conditions and hence, similar distribution patterns of environmental variables could be evidenced from this analysis (figures 10).

The first group included the years 2013, 2015, 2018 and 2019 characterised by high SST, high DefEpot (i.e. strong stratification), corresponding observations presenting positive scores along both axis 1 and axis 2 (dots in green and yellow). These warmer summers were also characterised by lower wind intensity, shallow mixed layer depth and lower phytoplankton biomass (with the exception of higher values in coastal waters), the wind and mixed layer variables are anticorrelated or not correlated to axis 2 (July wind $r = -0.99$ and depth mixed layer $r = -0.68$).

The second group included the remaining years: 2014, 2016 and 2017 located in the negative part of Axis 2 (dots in blue and purple). Summer of years 2014, 2016 and 2017 were characterized by high wind intensities, high surface salinities, and high turbidity near the coast, all these variables contributing to the structuration of axis 2 in its negative part. By opposition with the first group, years 2014, 2016 and 2017 were characterised by lower SST and some sectors (offshore) still presented a strong stratification of the water column (high values of DefEpot).

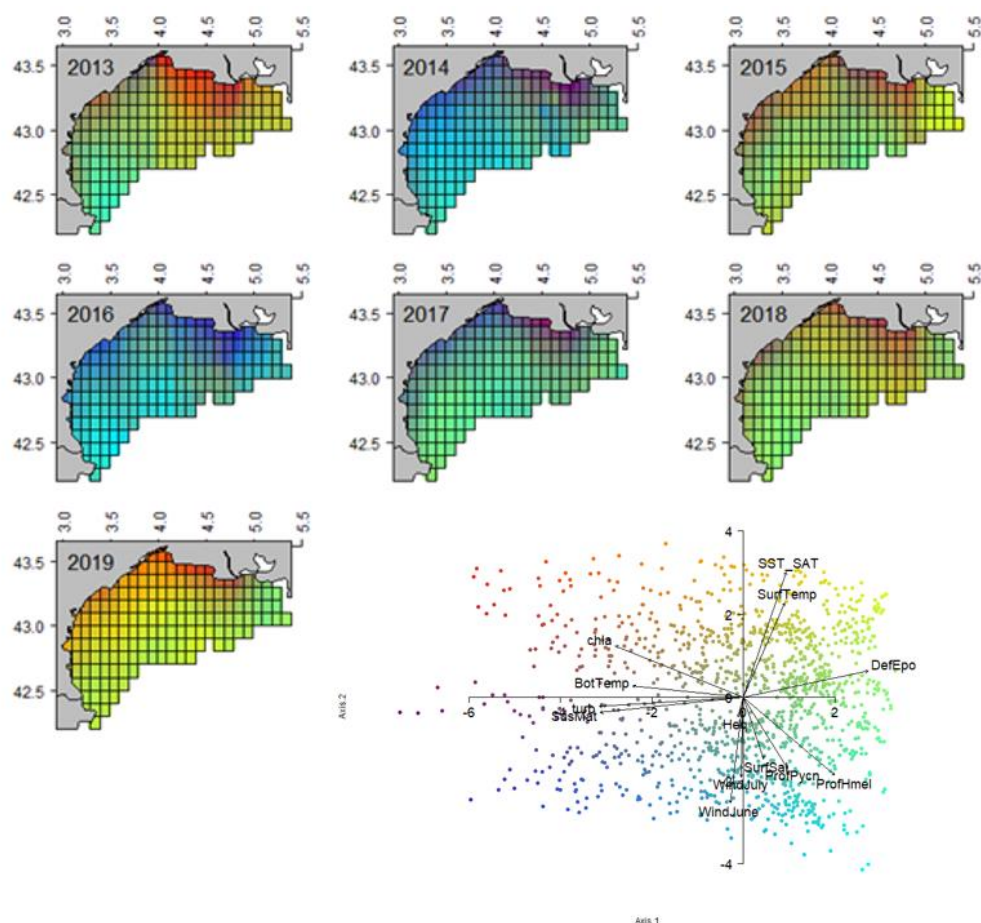


Figure 10: Spatial and temporal projection of PCoA axes of environmental data. Each dot in the scatter plots represents a grid cell position in the PCoA axes and the colours of these dots are identical to the mapped grid cell colours. The details of environmental variables contributions to the 1-2 plan of the PCoA analysis are presented using arrows (*envfit* analysis)

3.2- Interannual and spatial variability of copepod communities

3.2.1. Total copepods abundance

Considering total copepod abundance, there were no clear spatial patterns of distribution nor recurrent distribution pattern of abundance though some differences between years were noticeable (figure 11). For instance, summer 2013 was the PELMED survey during which the copepod abundance was the highest reaching mean value of $1605.52 \pm 831.72 \text{ ind.m}^{-3}$ compared to mean values ranging from $153.95 \pm 156.10 \text{ ind m}^{-3}$ in 2014 to $573.43 \pm 484.08 \text{ ind m}^{-3}$ in 2019. Summer 2015 was characterised by very low abundance near the Rhone plume reaching 5.50 ind m^{-3} . Such a distribution pattern of abundance was only recorded in 2015 and was opposite to the one observed in 2013. Small patches of higher abundance were observed in 2018 in the coastal area of the Gulf of Lion and in 2019, in the western southern part. The patterns observed correspond to the distribution of the tree main species (figure of copepods composition): *Oithona similis*, *Centropages typicus* and *Acartia clausi*. The maps of these species' abundance distribution are available in Appendix 4 to 6.

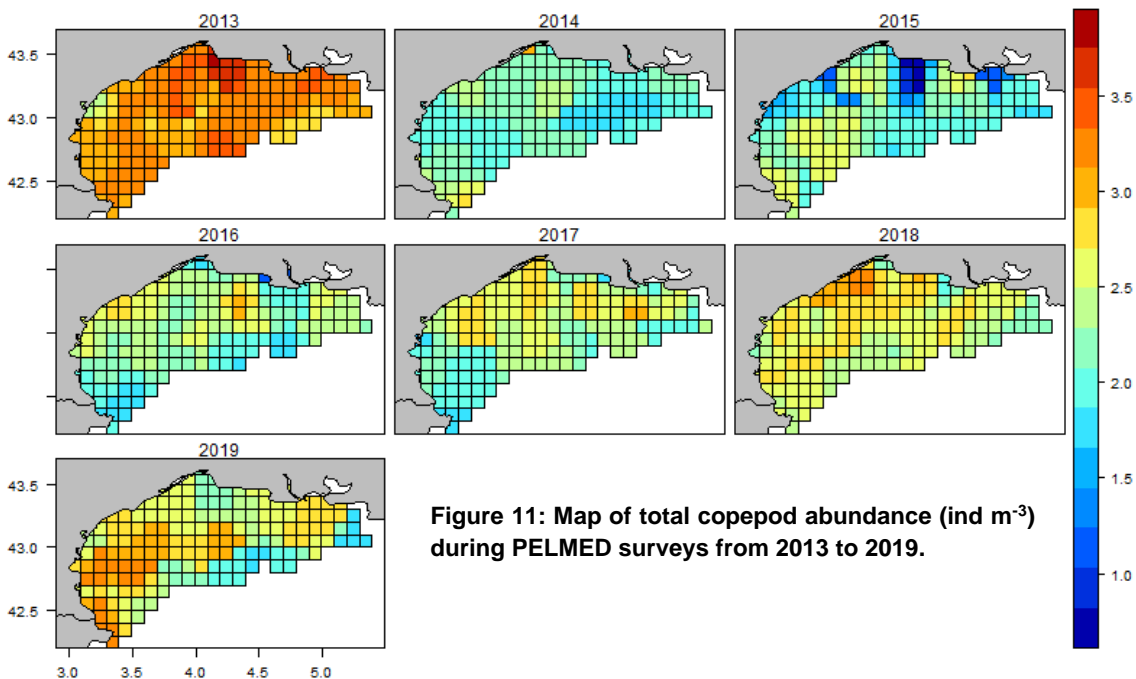


Figure 11: Map of total copepod abundance (ind m^{-3}) during PELMED surveys from 2013 to 2019.

3.2.2. Copepod assemblages : composition and interannual variability

The summer species composition through the years remained rather stable, even if small changes could be evidenced for specific years (Figure 12). In fact, the copepod community was always dominated by three major species namely *Oithona similis* (32% to 62% of total copepod abundance, depending on the year considered), *Acartia clausi* (8% to 27%) and *Centropages typicus* (7% to 27%). Secondary species from the genus *Oithona* (*O. plumifera*, *O. nana*) were always present over the 2013-2019 study period though representing less than 10% relative abundance. The same holds for *Nannocalanus minor*. Other species exhibited high interannual variability and were only observed during once or twice over the study period as exemplified by *Acartia danae* and *Centropages bradyi*

in summer 2016, and *Calocalanus pavo* (summer 2015 and 2016). Finally, species such as *Temora stylifera* were recurrently observed over the period 2014-2018.

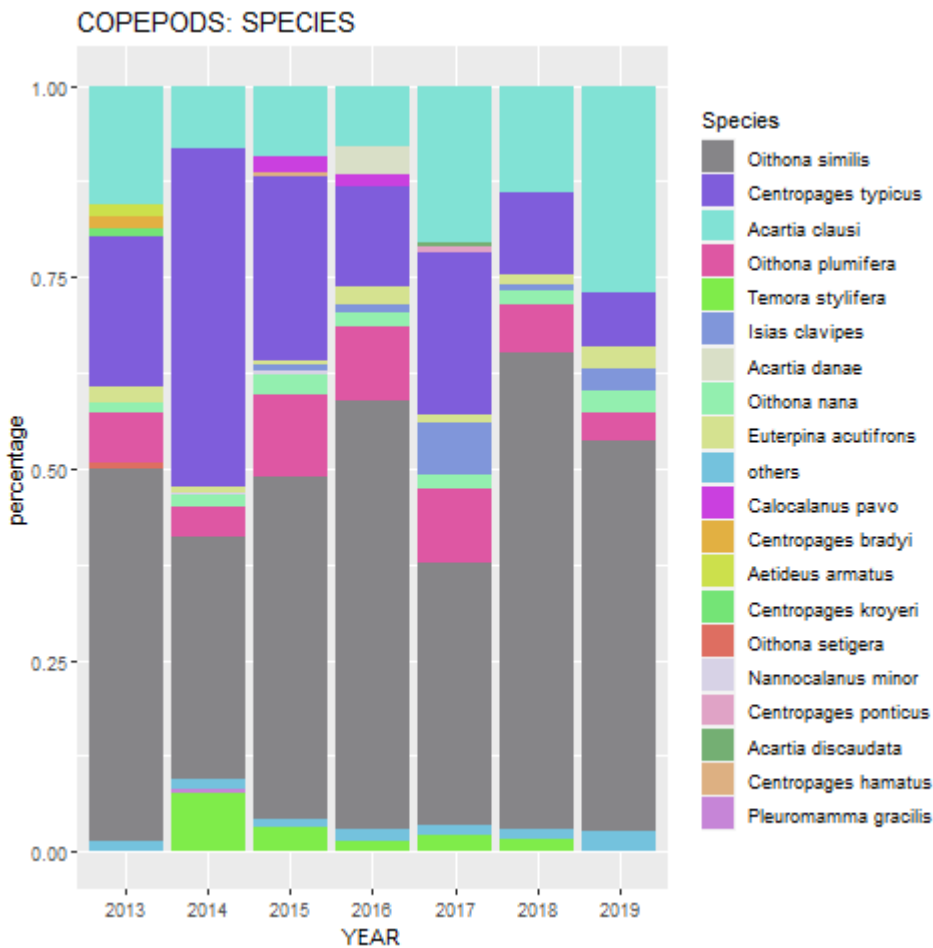
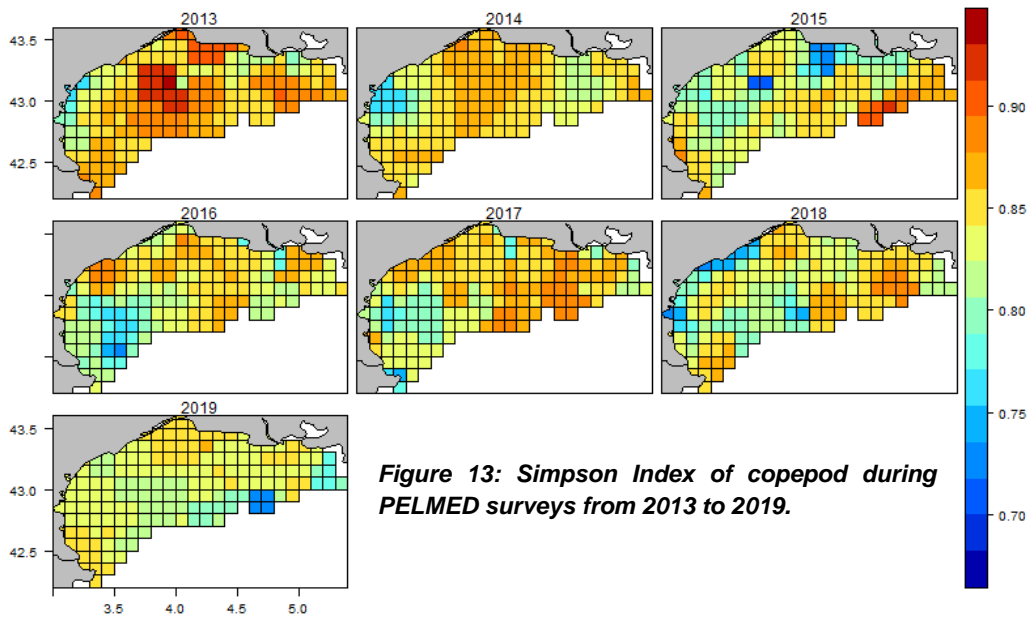


Figure 12: Barplot showing the relative abundance of the main copepod species in the gulf of Lion and their interannual variability

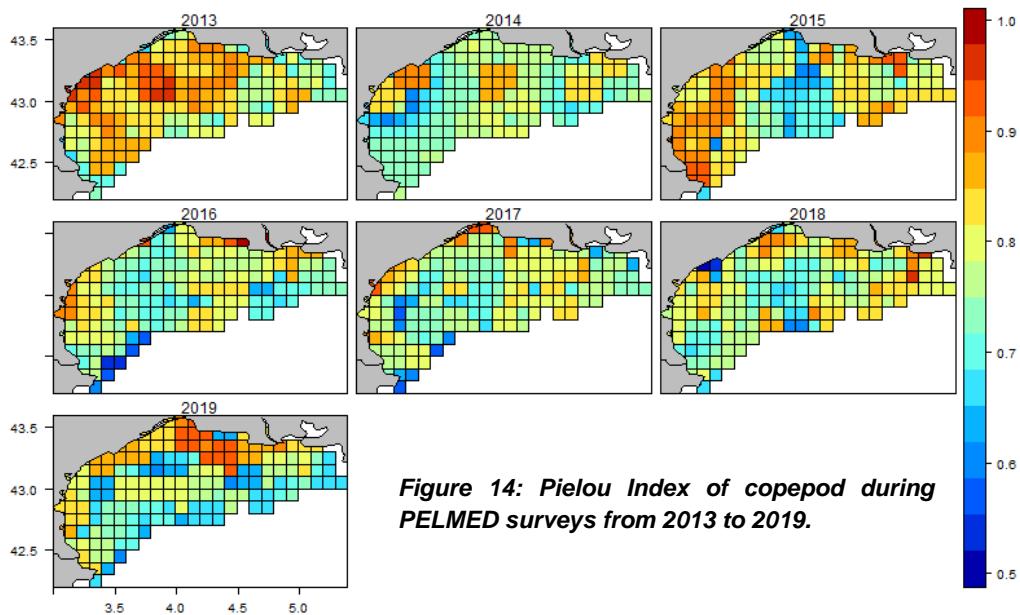
3.2.3- Copepod diversity

3.2.3.1 - Alpha diversity: Simpson index

Only maps of the Simpson index are presented here as the distribution patterns were more evidenced compared to other diversity indexes (see maps for other diversity indexes in Appendix 7 and 8). Simpson index distribution pattern was rather similar each summer over the study period, exception made of summer 2013 with always higher values at the eastern side of the GoL (0.82 to 0.93) , and lower values at the west (0.73 to 0.86). These lower diversity areas are located near the coast (2014, 2017 and 2018) or offshore (2015, 2016 and 2017). As for total copepod abundance distribution, summer 2013 showed a different spatial pattern compared to other summers with rather high Simpson index values in the central part of the Gulf of Lion (0.95) as well as in the dilution plume of the Rhone (0.92). Summer 2015 and 2019 were characterised with small areas of particularly low diversity (0.68 to 0.72), coinciding with low copepod abundances (figure 13; figure 11).



Pielou index distribution followed a reverse distribution pattern, with lower offshore values (0.5 to 0.85) compared to coastal waters with higher values reaching 1 (Figure 14). Pielou index was particularly high during summer 2013 (>0.7) and higher values distribution this year concerned almost the whole GoL, suggesting all copepod species were equally abundant within the copepod communities. For other years, the distribution of the Pielou index often decreased from west to east i.e. east communities abundances are more balanced than west ones.



3.2.3.2 - Functional beta diversity

Within the 7 functional traits considered in this study, 4 were chosen and were presented in the results section as they allowed to link copepod communities' composition to functional traits.

The functional trait "Max Length" showed recurrent distribution patterns with increasing gradient in maximal copepod length from the coastal to the offshore area. Near the coast the maximum copepod body size was in fact around 1.4 mm while further offshore, maximum size often exceeded 2 mm. A western-eastern gradient of increasing maximum length completed the inshore-offshore gradient, copepods often exhibiting higher maximum length in the eastern part of the sampled area. These gradients were particularly marked in 2015 and 2017 due to the presence of *Centropages typicus*, *Heterorhabdus papilliger*, *Pleuromamma gracilis*, *Nannocalanus minor* (appendix 6,7,8 and 9) for which maximum length reaches 2.65 mm. As for total abundance distribution and alpha diversity (figures 11, 13 and 14), distribution of copepod maximum length allowed the identification of the same two patches in the center of the GoL as well as in the dilution plume of the Rhone River during summer 2013. Summer of 2016, 2018 and 2019 were characterised with generally lower maximum length for copepods (mean maximum length value reached 1.45 ± 0.09 mm versus ranging from 1.46 ± 0.15 mm and 1.58 ± 0.10 mm for other years), i.e., when *Oithona similis* represented more than 50% of total copepod abundance (figure 15).

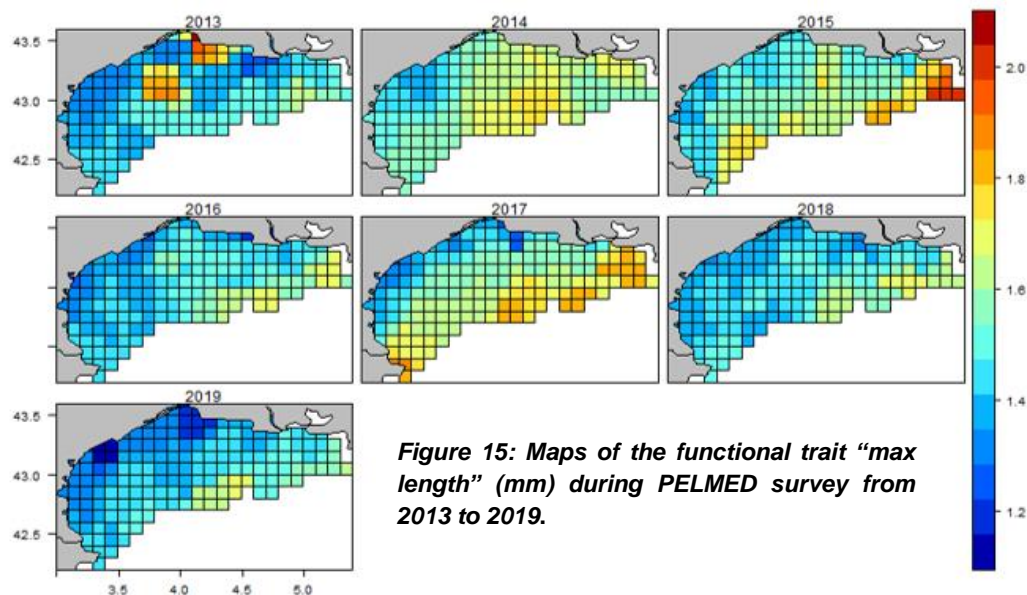


Figure 15: Maps of the functional trait "max length" (mm) during PELMED survey from 2013 to 2019.

The abundance distribution of Omnivorous-Herbivorous copepods was rather heterogeneous and did not totally match with total copepod abundance distribution, i.e. some of the species considered adopted other feeding strategies (e.g. carnivorous, omnivore only). This did not hold for patches of high values (red cells in summer 2016) corresponding to a copepod community comprising >50% omnivorous-herbivorous species. Generally, higher abundance of omnivorous-herbivorous copepods were observed in the coastal area and coincided with chl-a and turbidity distribution (Figure 16; Figure 9; Appendix 3).

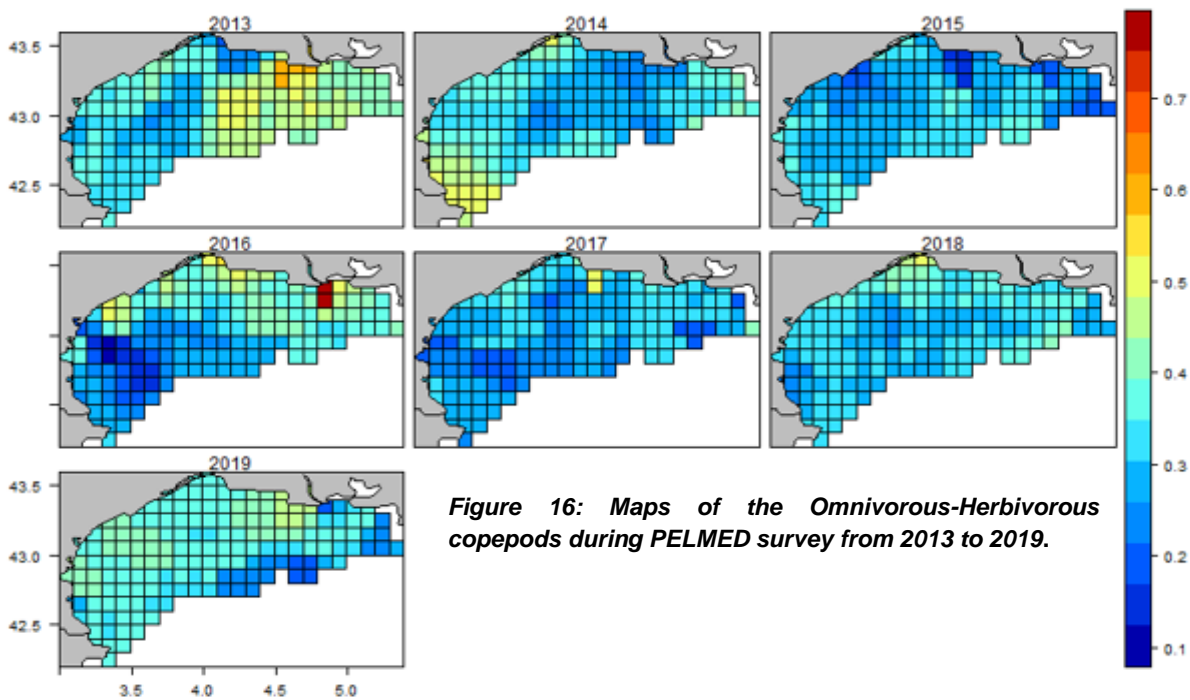


Figure 16: Maps of the Omnivorous-Herbivorous copepods during PELMED survey from 2013 to 2019.

Active ambush feeder functional traits distribution followed an opposite distribution pattern when compared to both maximum length (figure 15) and omnivorous-herbivorous (Figure 16). This distribution map of ambush feeders particularly matched the species distribution of *Oithona* spp., *Diaxis pygmaea* and *Haloptilus longicornis* (appendix 6, 12 to 16).

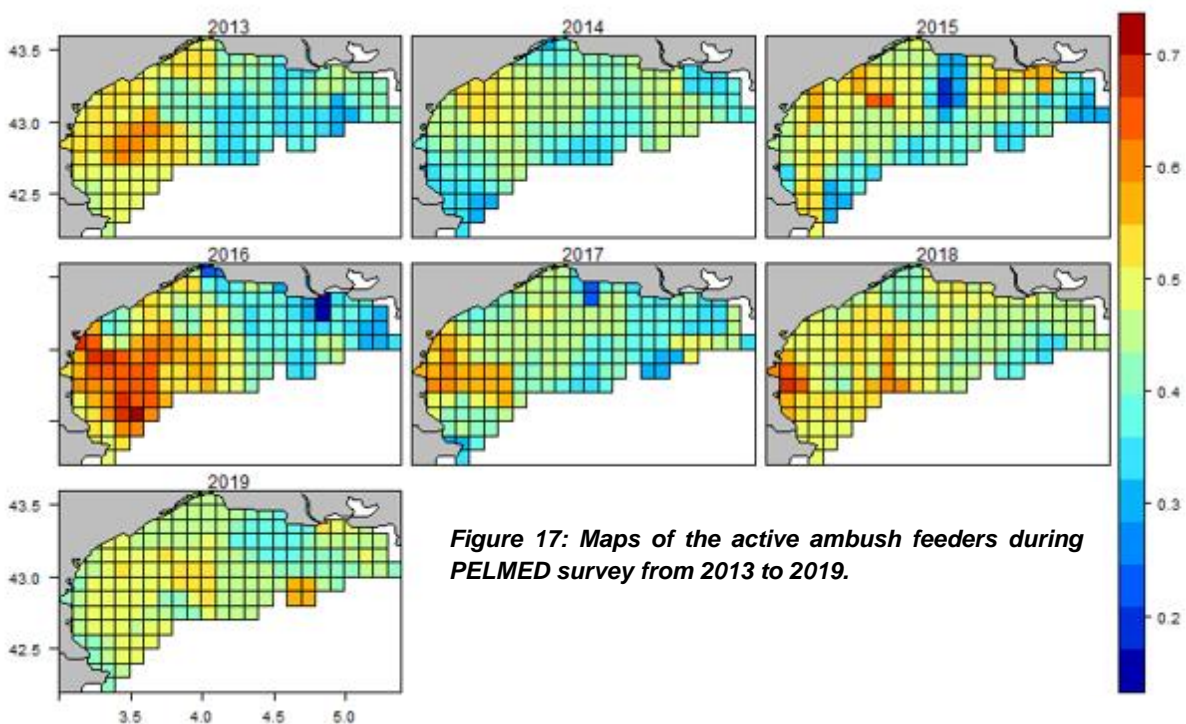


Figure 17: Maps of the active ambush feeders during PELMED survey from 2013 to 2019.

The proportion of copepods occupying the epipelagic zone was higher near the coast (reaching 88%) and at the western part of the GoL (reaching 78%), following Chl-a distribution (figure 9) and corresponding to copepod species of rather large size (figure 15). Offshore, only 45% of the copepod species under study were epipelagic.

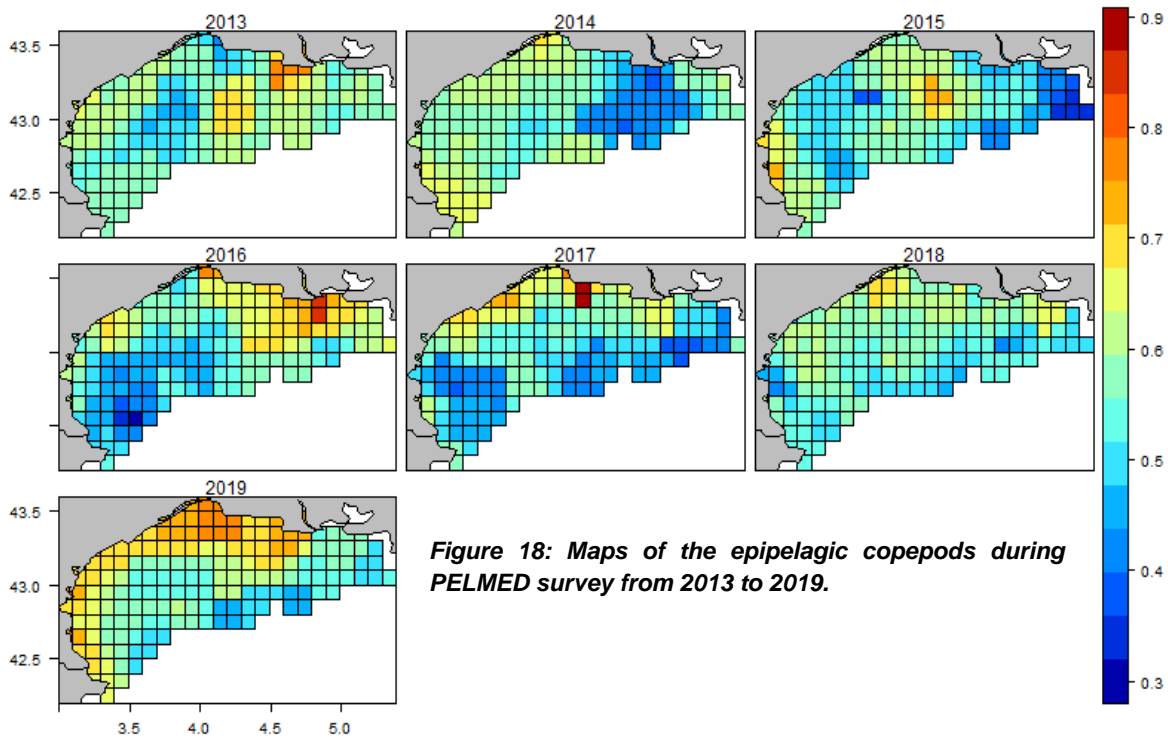


Figure 18: Maps of the epipelagic copepods during PELMED survey from 2013 to 2019.

Results from the RDA (Figure 19) synthesizes the spatial and temporal variability of the functional diversity based on the 7 functional traits considered. In the following figure, each dot in the scatter plots represents a grid cell assemblage and the colours of these dots are identical to the mapped grid cell colours. In other words, cells of the same colours present communities having similar functional traits regarding species composition. Two groups could be identified from this analysis.

The first group comprising summers 2013, 2014, 2015 and 2019 evidenced common trait distribution for copepods with a strong inshore-offshore gradient corresponding to the opposition of points along axis 1. This distribution matched the one observed for the copepod functional traits: maximum length, omnivorous-herbivorous feeding and the occupation of the epipelagic zone (figure 18).

The second group comprising summers of years 2016, 2017 and 2018 allowed to identify common functional traits in the western area of the GoL which corresponded to positive coordinates along axis 2 (green dots). This western patch coincided with the distribution pattern observed for active ambush feeders (figure 17) and confirm the opposition in copepod species and hence diets, size and distribution between these different years.

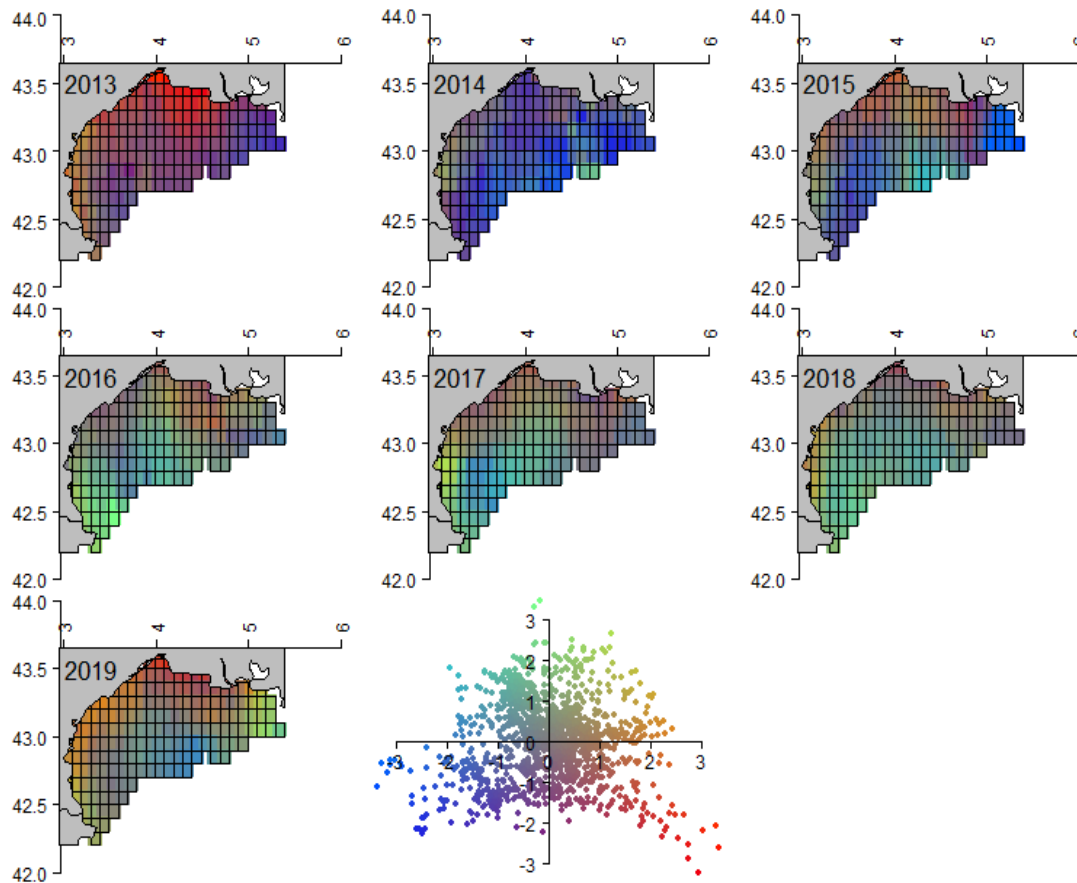


Figure 19: Spatial and temporal projection of RDA axes. Each dot in the scatter plots represents a grid cell position in the RDA two first axes and the colours of these dots are identical to the mapped grid cell colours.

3.2.3.3 - Relating copepod functional traits to environmental conditions

The first plan from the RDA analysis of community weighted means (CWM) explained 74.3% of the total variance of the dataset (51% for axis 1 and 23.3% for axis 2).

Axis 1 was structured in its positive part by the environmental variables: chlorophyll-a and suspended matters, both presented significant positive correlation coefficient with axis 1 (Table III; $r=0.52$ and 0.19 , respectively). Surprisingly, variables SST derived from satellite and the surface temperature originating from in situ data appeared to be opposite along axis 1 though they were not significantly correlated to axis 1 (Table III). These variables were associated with omnivorous-herbivorous copepods, occupying the epipelagic area and exhibiting weak vertical migration (figure 20). In its negative part, Axis 1 was structured by variables related to water column structuration namely the strength of the water column stratification (DefEpot; $r=-0.67$), the wind intensity in July ($r=-0.53$), the depth of the mixed layer (ProfHmel; $r=-0.47$) and surface salinity ($r=-0.23$). The latter variables were associated with copepods' diets 'omnivorous-detritivorous', their location in the epi-mesopelagic areas, these organisms exhibiting strong vertical migration (i.e. DVM behaviour). Axis 1 seems to represent the opposition between contrasting summer conditions of years 2013, 2014, 2015, and 2019 (marked by inshore-offshore chl-a gradients, strong stratification offshore versus strong mixing at the coast linked to salinity distribution) and years 2016, 2017, 2018 characterised by generally

higher salinity overall the sampled area, and both lower chl-a and suspended matter concentrations, particularly in mixed coastal waters. Offshore waters these summer years were marked by strong stratification, leading to a deepening of the mixed layer and occupied by ambush feeders exhibiting a variety of diets (either omnivorous-carnivorous, herbivorous or omnivorous).

Axis 2 was structured in its positive part by the following environmental variables: the surface salinity ($r=0.39$), the depth of the pycnocline (ProfPycn; $r=0.44$) and the depth of the mixed layer (ProfHmel; $r=0.28$), which were associated with omnivorous-carnivorous and omnivorous copepods exhibiting none or little vertical migratory behaviour, living in the epibathypelagic layer (0-4000m) and which were ambush feeders. In its negative part, Axis 2 was essentially structured by the equivalent water height (Heq; $r=-0.60$), and the chl-a concentrations ($r=-0.49$) which are associated with a weak vertical migration behaviour, an omnivorous-herbivorous diet and living in the epipelagic layer (0 - 200m). This axis 2 marked the opposition between stratified waters, characteristic of the years 2016, 2017 and 2018, in its positive part and the high standing stock of phytoplankton, during calm water conditions encountered during 2013, 2014, 2015 and 2019. Axis 2 confirms what the first axis pointed out, especially the strong inshore-offshore gradient. The positive part of the second axis seems to describe offshore waters whereas the negative part corresponds to the inshore area.

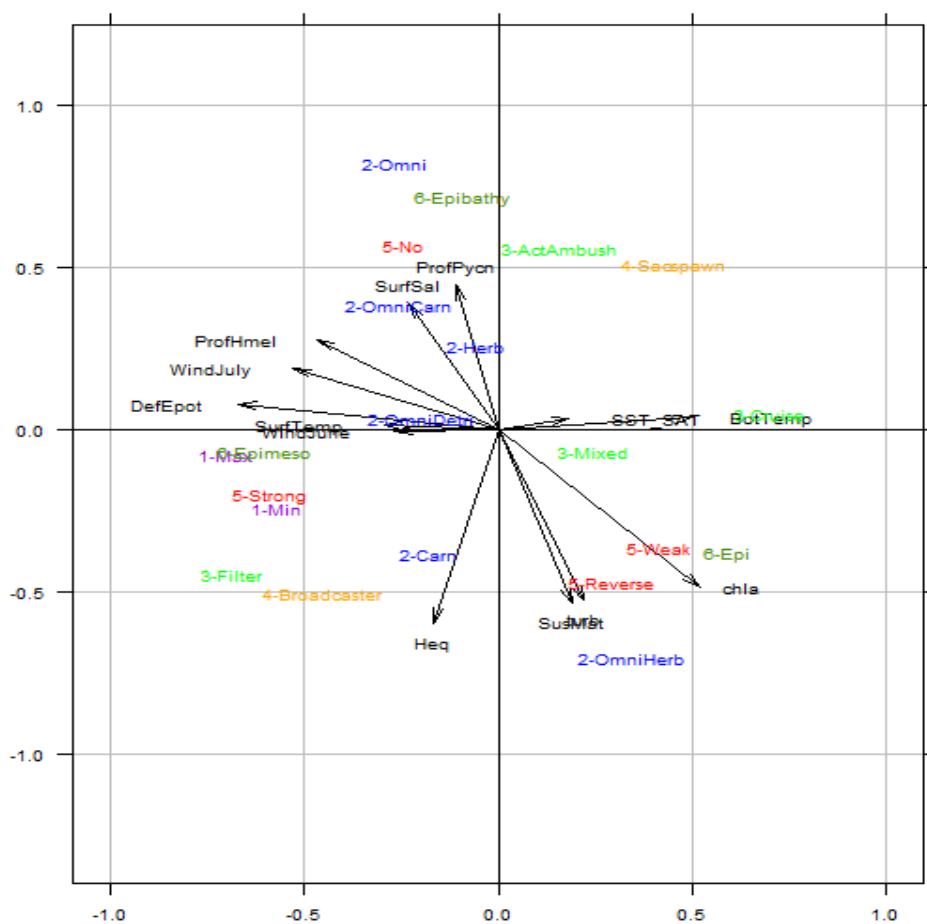


Figure 20: CWM-RDA axes and environmental variables correlation. In black environmental variables: ProfHmel, SurfSal, ProfPycn, SST_SAT, Chl-a, SusMat, turb, Heq, WindJune, SurfTemp, DefEpot and WindJuly. In color: purple: length min and max, blue: trophic regime, lightgreen: feeding strategy, orange: spawning strategy, red: dvm behaviour and green: pelagic layer.

Table III: Summary of the CWM RDA. The degree of association of each environmental variable with the two main axes (with their percentage contribution to the explained variance) is presented for the CWM-RDA. *In CWM-RDA, the environmental variables explained 21% of the total variation.

	CWM RDA		
	Axis 1	Axis 2	Variation*
	51%	23.30%	21%
Environmental variables			
BotTemp	0.50	0.04	
DefEpot	-0.67	-0.08	
Heq	-0.17	-0.60	
ProfHmel	-0.47	0.28	
ProfPycn	-0.11	0.44	
SST_SAT	0.18	0.03	
SurfSal	-0.23	0.39	
SurfTemp	-0.30	0.01	
WindJuly	-0.53	0.19	
WindJune	-0.27	-0.01	
Chl-a	0.52	-0.49	
SusMat	0.19	-0.54	
turb	0.22	-0.53	

4- DISCUSSION

4.1- Methodological considerations

4.1.1. - PELMED sampling design and impact on environmental and zooplankton dataset

In the first place, PELMED is an acoustic survey dedicated to pelagic fish stock assessments (see section 2.1.1). Optimisation of this DCF survey to suit Pelagic Habitats needs within the frame of the MSFD, and plankton sampling, should not interfere with the primary missions of PELMED. The PELMED sampling design explains the heterogeneity of our plankton dataset resulting in unbalanced numbers of samples between years and strong differences in sample spatial coverage. For example, in 2014, only 7 stations were sampled for zooplankton (e.g. WP2 net in figure 1). In 2014, the optimized surveys were not yet implemented, and it was a particularly windy year during July; these two facts may explain the very small number of samples collected. Strong wind conditions can in fact obstruct the use of acoustic for pelagic surveys and limit opportunities to deploy plankton sampling equipment. In case of bad weather conditions, priority was given onboard to the pelagic stock assessment and zooplankton samples were therefore not carried out.

Some numerical analyses, such as the comparison of communities at a given station over time, could not be performed given that the location and the number of hydrological stations could vary. This explains why several mapping methods were tested to project the observations on a common spatial grid. In the end, Block averaging (Petitgas et al., 2009; Petitgas et al., 2014) which was originally used for mapping pelagic fish distribution was proven to be also relevant for mapping zooplankton abundance and hydrological data. The use of the same method for both datasets make it possible to directly compare the distributions of pelagic fish and their potential prey. The advantage of block averaging is that data can still be mapped even if they have different spatial scales and samples with different locations. Interannual analysis of zooplankton variability was also complicated by the relative shortness of our time series (7 years) which makes it difficult to state whether observed changes in communities were due to the environmental conditions at the moment of the sampling or if the entire zooplankton community was affected by deeper changes at a longer time scale. In the framework of the MSFD, changes in the plankton community are observed over a 6-year period and compared to

6 years of reference. Generally, long term changes in plankton communities are inferred from a period of over 10-15 years (e.g. Beaugrand, 2003).

Samples were collected over the survey duration; thus, temporal scale should also be considered as another source of artifacts as there was systematically \cong 1 month's duration between the first and the last sampling. The fact that some environmental variables were averaged over the whole month of July whereas zooplankton abundances were those recorded at the moment of sampling, may have introduced a time scale bias making it difficult to directly link environmental variables with abundance data. Despite this difference of scales, the results showed relationships between environmental variables and zooplankton communities (section Results). The fact that some data were averaged allows us to integrate a known variability in our study. The choice of the summer period in our work allowed us to consider both strong environmental (e.g. water stratification, punctual freshwater inputs) and biological features (low primary production; d'Alcalà et al., 2004; Siokou-Frangou et al., 2010) that were likely to impact zooplankton community structure and distribution. As summer primary production is rather associated with nutrients regenerated inside the surface layer through microbial loop activity (Herrmann et al., 2014), the summer period also corresponded to a particular functioning of the plankton ecosystems.

4.1.2. - Zooplankton functional traits definition

Working on functional traits has several interests. Firstly, the functional trait-based approach deals with the complexity of marine ecosystems and describes the structure and the function of communities in a simple way (Brun et al., 2016). Ecosystem functioning and stability are mainly driven by environmental conditions, species traits and their biomass. The functioning of an ecosystem can thus be better characterized through the functional trait of its communities compared to a species-centric description of ecosystems (Kjørboe et al., 2018). Secondly, functional traits are general and universal. Indeed, functional groups are representative of a certain habitat or ecosystem, with a particular function, whereas taxonomic composition is representative of a given region (Hemingson and Bellwood, 2016). So, two different regions of the globe could have the same ecosystem functions, because of a similar habitat, but if only the taxonomic diversity is investigated, the differences and similarities would be harder to identify.

Species with similar functional traits are responding in a similar way to environmental and anthropogenic pressures and could be classified into functional groups. These groups could be used to study the effect of environmental changes or to describe functional diversity of zooplankton (Barnett et al., 2007; Pomerleau et al., 2015). For example, the study of key traits, such as the body size of marine copepods has highlighted latitudinal global patterns, confirmed the temperature-size relationship, and unveiled association between these traits and environmental conditions, such as temperature, water column transparency, chlorophyll seasonality or phytoplankton size (Brun et al. 2016). Functional trait-based approach can be used as an indicator to assess the restoration of a degraded ecosystem and see if the ecosystem retrieves its ecological functions (Josué et al., 2021). Finally, the temporal and spatial distribution of traits could be used to identify hotspots of functional diversity and study the responses of organisms to environmental changes, in order to determine areas for biomonitoring and trait-based conservation (Martini et al., 2021).

The PELMED dataset is adapted to a functional trait-based approach because species are identified at the finest taxonomic level and the traits for those species have been studied through literature (Kjørboe, 2011; Benedetti et al., 2016; Brun et al., 2016). These traits have been used because they cover several ecological functions (Litchman et al., 2013), they are ecological meaningful (Kjørboe, 2011; Kjørboe et al., 2015) and are commonly used for zooplankton (Barnett et al. 2007; Pommerlau et al. 2015; Benedetti et al. 2016; Brun et al. 2016). These traits are the most easily identified for any aquatic organisms, especially morphological traits, such as body sizes, which are easy to measure (Martini et al., 2021).

In order to have as many species as possible for the analysis, all the functional traits had to be complete as species with a missing functional trait could not be kept. So, when one or two traits were missing they were completed depending on the following two hypotheses: (1) “two species of the same genus share the same functional trait” and (2) “two species in the same functional group (Benedetti et al. 2018) share the same trait”. These assumptions could be false, and they could have introduced some bias by associating the wrong trait to a given species. Then in the analysis we carried out, the filled-trait could appear dominant in certain parts of the GoL but this could be artificial. In the present work, six species (of 43 copepod species) were concerned by these assumptions but only two of them were part of the 99% most abundant copepod species namely *Oithona similis* and *Isias clavipes*. Concerning *O. similis* the DVM behaviour was supposedly “weak” so as to be congruent to other *Oithona spp.* (completed by Benedetti et al. 201). For *Isias clavipes*, the reproduction strategy was assumed to be “sac-spawner” based on the clustering Benedetti et al., (2018). Therefore, our results could have been affected by these assumptions, particularly since *O. similis* was the most abundant species in the GoL and its traits will have more weight in our analysis. Though we are aware that attributing the same trait to congeneric *Oithona* species is not wrong, we have to keep in mind the contribution of this species to total abundance and therefore to observed trends in our results. A solution to reduce the potential bias related to these assumptions would be to reduce the weight of species having “assumed” traits in analysis. The optimal way to complete this information would be to complete the functional trait database by conducting experimental studies targeting feeding, reproduction, and migration on species for which uncertainties remain. Another limit encountered in our functional trait analyses is the possible misrepresentation of the functional trait “herbivorous trophic regime” and “reverse DVM behaviour”. Indeed, these traits were represented by one species each. This particularly holds for the “herbivorous” as another similar trait was also considered: “omnivorous-herbivorous”.

4.2- Summer environmental conditions during PELMED surveys over the period 2013-2019

Almost for every environmental variable, an inshore-offshore gradient and an east-west have been observed, especially for SST (lower near the coast), salinity (lower near the coast), chlorophyll-a concentration (greater near the coast) and the deficit of potential energy (lower near the coast). These results reflect less stratified and more productive waters near the coast, which is totally congruent with the general hydrographical features of the GoL and linked to the effect of the Rhone water plume. The latter corresponds to a thin layer of nutrient-enriched waters exhibiting lower salinity (33, Brasseur, 1991) compared to oceanic part of the GoL (up to 38.2, Brasseur, 1991; Kouwenberg, 1994). The high chlorophyll-a and suspended matter concentration along the coast is therefore mostly due to the Rhone inputs, which were reported to be responsible for 20 to 40% of the Chl-a concentration on the shelf, with a decreasing gradient from East to West (Macias et al., 2018). Offshore, the temperature increase in summer generally results in an increase of the water stratification and a decrease of the production as reported in previous studies (Sarmiento et al., 1998; Bopp et al., 2001; Behrenfeld et al., 2006).

These environmental gradients have also been pointed out in the literature (Gaudy et al., 2003; Pisano et al., 2020) and result from the combination between river inputs and wind regimes (Espinasse et al., 2014). In fact, the wind regime could dispatch the Rhone plume along the coast and bring the production to the west coast (Demarcq and Wald, 1984). Qiu et al (2009) suggested that the transport and distribution of particles are strongly related to the hydrodynamics structures (e.g. surface waters mixing according to a cyclonic current ;Milot and Taupier-Letage, 2005), particles spreading almost anywhere in the GoL.

Among the seven years studied, interannual variability has been observed and two groups of years were highlighted by applying a multivariate analysis to hydrological data. The first one included the summers of 2013, 2015, 2018 and 2019 which were warmer compared to other years, especially in 2019 when surface temperature reached 24.64°C and even offshore where it did not go below

21.35°C. The low salinity, the low intensity of the wind, especially in 2013, and the shallow mixed waters characterized these years. The second group was composed of the remaining years 2014, 2016 and 2017. The environmental conditions that characterize these years were the strong wind, especially in 2014, slightly lower temperature, and high salinity (value range: 36.76 to 38.21 for 2018 and 2019), low potential energy deficit and a higher chlorophyll-a concentration in offshore areas. These years the waters were turbulent, not stratified and well mixed.

Hydrodynamic conditions in the gulf of Lion were demonstrated to significantly influence the distribution and availability of nutrients and therefore drive the distribution and the population dynamics of both primary producers and higher trophic levels (e.g. zooplankton; Espinasse et al. 2014). Though wind intensity varied between years, wind direction was always the same, and corresponded to the strong and cold wind coming from the northwest, the “Tramontane”. The Mistral is also a strong wind blowing in the gulf of Lion and both winds dominate water movements, influencing coastal upwellings, mixing of fresh and saline waters (Cruzado and Velasquez, 1990) and surface current direction (Millot and Taupier-Letage, 2005). They could cause intense surface water cooling (Jiang et al., 2003; Sicre et al., 2016) as exemplified by our results, which showed colder summer years coincided with the most intense winds.

4.3- Summer copepod communities: composition, functional diversity and spatial and interannual variability

4.3.1. - Structure of summer zooplankton communities

Mediterranean zooplankton communities exhibit an important seasonality. In fact, spring is considered the most productive period for zooplankton (Siokou-Frangou et al., 2010; Fullgrabe et al., 2020). The winter and spring communities are generally dominated by calanoid copepod such as *Clausocalanus* spp., *Paracalanus* sp., and *Centropages typicus*, whereas the summer and autumn communities are essentially composed of cycloid copepods (as *Oithona* spp.) and cladocerans (Calbet et al., 2001; Fernández de Puelles and Molinero, 2008; Fullgrabe et al., 2020). Fullgrabe et al. (2020) have also found that in summer a majority of carnivorous groups such as siphonophores, scyphozoan larvae, fish larvae and chaetognaths and mostly large size organisms dominate zooplankton communities. Amongst omnivorous zooplankton *Oithona nana* generally represents a high proportion of the community in summer due to their capacity to adapt to different prey types such as phytoplankton, ciliates or detritus (Calbet et al., 2001; Atienza et al., 2006).

In our study, *Oithona nana* was the 8th most abundant species (out of the 43 species considered) while copepod communities were dominated by *Oithona similis* (32% to 62% of total copepod abundance, depending on the year considered), *Acartia clausi* (8% to 27%) and *Centropages typicus* (7% to 27%). *C. typicus* is a temperate species indigenous to the temperate Atlantic, the North Sea and the Mediterranean Sea (Rose, 1933), accounting for between 10 and 50% of total copepod numbers (Ianora and Buttino, 1990; Ianora, 1998). Usually *C. typicus* occurs in spring (Calbet et al 2001) but its presence during summer is also not surprising (e.g. (Kouwenberg, 1994). *A. clausi* is a coastal species frequently observed throughout the year in coastal areas of the Gulf of Lion, particularly in waters under the influence of the Rhone river plume (Kouwenberg, 1994; Nowaczyk et al., 2011) as exemplified by our map of abundance for this species in summer 2013. The dominance of Mediterranean copepod communities by *Oithona* spp is not rare (e.g. Gaudy et al. 2003; Nowaczyk et al. 2011), this small species was indeed reported to thrive in summer in different sectors of the Mediterranean Sea at a larger scale.

Interannual variability of copepod species abundance and composition was also not surprising and already observed over interannual surveys (e.g. Christou, 1998), in relation to interannual variability of forcing parameters (e.g. temperature and salinity). In our case, the summer copepod species composition through the years remained rather stable. Rare species such as *Acartia danae*,

Centropages bradyi and *Calocalanus pavo* exhibited were only observed once or twice over the study period and contributed to the overall high interannual variability.

Finally, it should be remembered that only adult stages were considered in our analyses, given our aim was to relate functional stabilized traits to environmental conditions. Therefore, the dominance of copepod communities by *O. similis*, *A. clausi* and *C. typicus* did not consider copepodite stages which comprised a non-negligible proportion of *Paracalanus* spp., and *Temora stylifera*. This could explain the differences that could be observed between our copepod communities composition and previous studies (e.g. Kouwenberg 1994; Gaudy et al. 2003; Nowaczyk et al. 2011), evidencing the summer dominance of *T. stylifera* and *P. parvus* in the GoL.

4.3.2. - Copepods spatial variability during summer

Considering the overall copepods community, no clear spatial pattern or gradient can be deduced through years but the distribution of total copepod abundance depended mainly on *O. similis*, *C. typicus* and *A. clausi* abundance. In this study *C. typicus* was more abundant in offshore areas, its abundance near the coast was almost zero. This is congruent with what is known from this species, generally spending the summer period below the thermocline in oceanic waters (Kouwenberg 1994). *A. clausi* and *O. similis* were more abundant near the coast, in conformity with their coastal and neritic preferences. However, *O. similis* showed a ubiquitous distribution in 2013 by having a high abundance in the whole gulf of Lion. 2013 is a year marked with a weak wind, so it could explain the change of distribution for *Oithona similis* but also why a higher general abundance for copepod communities was observed. Probably as a consequence of the weak wind, the chlorophyll-a concentration was higher in 2013 as vertical mixing may enhance primary production and then zooplankton biomasses (Donoso et al, 2016). Castellani et al. (2016) showed that there was a positive and significant relationship between *O. similis* abundance and Chl-a concentration. *O. similis* is also part of the copepods with the lower maximal length (1.20 mm) and the lower minimal length (0.43 mm). The small size could explain why this species is particularly responsive to hydroclimatic events.

Even if there are no recurrent spatial patterns of distribution for the whole copepod community, some areas of the gulf showed differences between years: near the Rhone plume and in the western part. These differences in abundance could be explained by specific environmental conditions in these areas. Such ecoregionalisation of the GoL with different copepod assemblages occupying different sectors was already demonstrated by Kouwenberg (1994) and confirmed by Espinasse et al. (2014). It appeared to be linked to both the main hydrodynamic features of the area and to more local processes. Consequently, in 2013, near the Rhone plume abundance was higher than everywhere else in the gulf but in 2015 it was the opposite, i.e. abundance was lower than everywhere else. The Mediterranean Sea is characterized for being an oligotrophic basin except in large estuaries such as the gulf of Lion, where the Rhone is known to be responsible for the most part of the productivity of the western Mediterranean. The Rhone is typically bringing nutrients in the east part of the Gulf (Lochet and Leveau, 1990; Millot, 1990; Siokou-Frangou et al., 2010) but depending on the wind conditions the plume can impact the western part of the gulf (Demarcq and Wald, 1984; Fraysse et al., 2014) and hence, copepod distribution. Finally, environmental variables alone cannot always explain the distribution of the community (e.g. Nowaczyk et al. 2011), and other factors have to be considered while studying copepod communities over a dedicated season. Yebra et al (2020) showed that in the western Mediterranean, zooplankton biomass decrease was not only due to environmental conditions but also to predation by *Sardina pilchardus*. So further investigations are needed to link the pelagic fish data collected during PELMED with the results obtained here.

Except for the three main species of copepod considered above, there was no clear spatial gradient or pattern in species distribution during summer. This is probably due to the fact that most copepod species in the GoL are eurythermal and euryhaline, therefore tolerating a wide range of variability in hydrological conditions. Zooplankton spatial variability is indeed generally associated with seasonal

changes in hydrodynamic features and circulation patterns (Kowenbergh 1994). By considering the functional traits, distribution patterns and gradients clearly appeared from inshore to offshore and from east to west (figure 19).

4.3.3. Copepod functional traits and environment relationships

Rather than a species-based approach, a community-based approach was chosen in order to see the response of average trait expressions of communities to environmental gradients. In the framework of the MSFD (i.e. regarding the need to consider plankton communities at different levels of ecological integration from functional groups to species) but also to study the variability of the functional diversity, the community based approach was the most suited. In fact, it can easily take into account intraspecific variation in trait expression across populations (Garnier et al., 2007). In addition, species do not need to be identified as long as the functional traits are filled out although it is not possible to assess how a single species responds to environmental changes (Kleyer et al. 2012), i.e. if a rare species is impacted by a specific environmental change.

The RDA analysis summarizes the information and makes it possible to link the functional traits with environmental variables. The mapping of the RDA axes using an RGB colour scheme allowed also to put the RDA result into spatial and temporal context and facilitate the identification of trends. The RDA seemed to discriminate between the different conditions in summer (i.e. temporal trends) and to highlight the inshore-offshore gradient (i.e. spatial trends). The results make it possible to identify particular areas with different ecosystem functioning.

Summers 2013, 2014, 2015 and 2019 characterized by important freshwater inputs (Heq) and both high Chl-a and suspended matter concentrations were associated with the omnivorous-herbivorous copepods, occupying the epipelagic area, exhibiting weak vertical migration which were mostly suspension feeders. This result is congruent with previous studies demonstrating the western Mediterranean basin to be dominated by small and medium (<1.5mm prosome length) herbivorous/omnivorous copepods (i.e. *Acartia clausi*), the species being associated to nanophytoplankton-rich conditions (Pinca and Dallot, 1995; Gaudy et al., 2003; Alcaraz et al., 2007).

By contrast, summers 2016, 2017 and 2018 characterized by strong winds and a strong stratification (in offshore areas) were associated with large copepods (i.e. with a high maximum and minimum length) occupying the epimesopelagic layer exhibiting no preferential diet. As previously discussed, this pattern matched the abundance distribution of the dominant copepod species *C. Typicus*. This also holds for large size copepod species contributing to a lesser extent to total copepod abundance namely *Heterohabdus pappiliger*, *Pleurommama gracilis* and *Nanocalanus minor* (Appendix 9 to 11).

Our results allowed us to discriminate the inshore coastal ecosystem characterized by high chl-a and suspended matter concentration and freshwater input associated with omnivorous-herbivorous copepods, which have a weak DVM behaviour and live in the epipelagic layer. Copepod feeding activity depends on a variety of factors among which prey types, sizes and concentrations (Frost, 1972). Therefore, it is not surprising that in sectors presenting surface patches of chl-a and suspended matter, most copepods were omnivorous-herbivorous. Offshore waters masses are strongly stratified, and copepods may likely occupy different layers of the water column as already evidenced by Kowenbergh (1994) for *C. typicus* and as shown from our results as most species lived in the epibathypelagic layer and presented no DVM behaviour. Oceanic species rely on various diets and active ambush feeding behaviour to encompass the vertical heterogeneity of food resources distribution, linked to stratification. The copepod size distribution pattern we observed in summer is congruent with other published studies (e.g. Espinasse et al 2014; Nowaczyk et al. 2011).

Surprisingly, the RDA depicted an opposition (along Axis 1; see figure 20) between the SST derived from satellite data and the surface temperature coming from the PELMED survey (surftemp). This could be explained by the sampling design of PELMED as explained in section 2.1.1 regarding

temporal scale. The patterns obtained from the RDA are slightly different from those obtained from the PCoA of environment variables (figure 10 and figure 19). Years were regrouped in a slightly different way depending on the analysis: environmental conditions only *versus* functional traits constrained by environmental variables. This could be explained by methodological differences between these two methods, as RDA can be considered as a constrained version of ordination, wherein canonical axes - built from linear combinations of response variables - must also be linear combinations of the explanatory variables.

Before concluding, it is also important to point out that this analysis of the relationships between copepod functional traits and environmental conditions does not include all the possible variables that can explain these relationships. For example, adding meteorological data such as precipitation, irradiance and atmospheric pressure could complete the description of the environmental conditions. Another parameter to explore (once the time series becomes longer) is the Northern Atlantic Climate (NAC) which can impact the western Mediterranean ecosystem. Molinero et al. (2008) indeed demonstrated a significant relationship between the intensity and variability of the NAC and the long-term changes of zooplankton functional groups. Plankton is known to follow a seasonal dynamic and the past events influence today's communities. Therefore, integrating information with a time lag (*i.e.* during the spring bloom) could provide a better understanding of the summer zooplankton communities and the drivers of their spatio-temporal variability. In addition to environmental variables, biotic drivers such as interactions between different trophic levels, predation pressure or trophic competition could also be investigated (e.g. Yebra et al., 2020).

5. CONCLUSION AND MONITORING PERSPECTIVES

Strong environmental gradients from the coast to the oceanic region offshore and from the west to the east of the GoL have been identified. In addition to this spatial variability, an interannual variability in the environmental conditions have also been observed. The distribution of the zooplankton community and their functional traits seem to be related to the spatial and temporal variability of the considered environmental conditions.

In addition to a strong diversity and evenness, summer copepod communities were characterized by three dominant species, namely *Oithona similis*, *Centropages typicus* and *Acartia clausi* which drive the distribution of community-weighted mean trait values. The analysis of trait–environment relationships allowed the identification of two main summer communities. The first one is a coastal community characterized by a Omnivorous-Herbivorous diet, living in shallow and well mixed waters rich in chlorophyll-a and the second is an offshore community, living in more stratified waters characterized by an absence of vertical migration behaviour, an active ambush feeding strategy. The analysis points out some locations as the Rhone plume, the southwest coast of the gulf, and the offshore area, which have different functional compositions, so probably different ecosystem functioning.

Interannual variability has also been observed within zooplankton communities, mainly due to the stratification of the waters induced by hydrological events such as wind, temperature and salinity. Some years were more stratified than others. Stratification is partly a consequence of the temperature increase *i.e.* global warming and wind regimes. So knowing the functional groups and zooplankton communities living in stratified waters is a prerequisite for the development of good environmental indicators within the MSFD. Thus, knowing the distribution of community-weighted mean trait values in the gulf of Lion could provide key information about pelagic habitats and their ecological state.

This study provides an exploratory analysis on a 7 years time-series and explores in which direction and what could be done with this dataset. To be able to observe a clear interannual variability, more years will be needed. More analysis including the phytoplankton could be required in order to have a

better understanding of the dynamic of plankton communities in gulf of Lion as well as the link between zooplankton and phytoplankton

The PELMED survey is the only source of information that brings observations about plankton communities in the whole gulf of Lion, including coastal and offshore areas. This exploratory analysis of the PELMED dataset clearly shows the potential of this survey to provide an assessment of the good environmental status of Pelagic Habitats, but more data and analyses will be needed. In order to improve the monitoring, having seasonal or a spring observations of plankton communities will be useful. It is known that the species are different between spring and summer, so studying the functional diversity during spring could be interesting as well. Although an additional long-term spring survey may raise some feasibility issues, it remains the ideal option. However, a more feasible and less costly alternative would be to combine the large extent observations of the PELMED survey with zooplankton observations collected in fixed station in the Gulf of Lions on a weekly basis as part of MOOSE monitoring networks such as the fixed station DYFAMED, ANTARES and MOLA.

REFERENCES

- d'Alcalà MR, Conversano F, Corato F, Licandro P, Mangoni O, Marino D, Mazzocchi MG, Modigh M, Montresor M, Nardella M, et al** (2004) Seasonal patterns in plankton communities in a pluriannual time series at a coastal Mediterranean site (Gulf of Naples): an attempt to discern recurrences and trends. *scimar* **68**: 65–83
- Alcaraz M, Calbet A, Estrada M, Marrasé C, Saiz E, Trepát I** (2007) Physical control of zooplankton communities in the Catalan Sea. *Progress in Oceanography* **74**: 294–312
- Atienza D, Calbet A, Saiz E, Alcaraz M, Trepát I** (2006) Trophic impact, metabolism, and biogeochemical role of the marine cladoceran *Penilia avirostris* and the co-dominant copepod *Oithona nana* in NW Mediterranean coastal waters. *Mar Biol* **150**: 221–235
- Bănaru D, Mellon-Duval C, Roos D, Bigot J-L, Souplet A, Jadaud A, Beaubrun P, Fromentin J-M** (2013) Trophic structure in the Gulf of Lions marine ecosystem (north-western Mediterranean Sea) and fishing impacts. *Journal of Marine Systems* **111–112**: 45–68
- Barnett AJ, Finlay K, Beisner BE** (2007) Functional diversity of crustacean zooplankton communities: towards a trait-based classification. *Freshwater Biology* **52**: 796–813
- Baudrier J, Lefebvre A, Galgani F, Saraux C, Doray M** (2018) Optimising French fisheries surveys for marine strategy framework directive integrated ecosystem monitoring. *Marine Policy* **94**: 10–19
- Beaugrand G** (2003) Long-term changes in copepod abundance and diversity in the north-east Atlantic in relation to fluctuations in the hydroclimatic environment. *Fisheries Oceanography* **12**: 270–283
- Beaugrand G, Kirby RR** (2010) Climate, plankton and cod. *Global Change Biology* **16**: 1268–1280
- Bedford J, Ostle C, Johns DG, Atkinson A, Best M, Bresnan E, Machairopoulou M, Graves CA, Devlin M, Milligan A, et al** (2020) Lifeform indicators reveal large-scale shifts in plankton across the North-West European shelf. *Global Change Biology* **26**: 3482–3497
- Behrenfeld MJ, O'Malley RT, Siegel DA, McClain CR, Sarmiento JL, Feldman GC, Milligan AJ, Falkowski PG, Letelier RM, Boss ES** (2006) Climate-driven trends in contemporary ocean productivity. *Nature* **444**: 752–755
- Benedetti F, Gasparini S, Ayata S-D** (2016) Identifying copepod functional groups from species functional traits. *Journal of Plankton Research* **38**: 159–166
- Benedetti F, Vogt M, Righetti D, Guilhaumon F, Ayata S-D** (2018) Do functional groups of planktonic copepods differ in their ecological niches? *Journal of Biogeography* **45**: 604–616
- Bopp L, Monfray P, Aumont O, Dufresne J-L, Treut HL, Madec G, Terray L, Orr JC** (2001) Potential impact of climate change on marine export production. *Global Biogeochemical Cycles* **15**: 81–99
- Bourdeix J-H** (1985) PELMED - PELAGIQUES MEDITERRANÉE. doi: 10.18142/19
- Brasseur PP** (1991) A variational inverse method for the reconstruction of general circulation fields in the northern Bering Sea. *Journal of Geophysical Research: Oceans* **96**: 4891–4907
- Brun P, Kiørboe T, Licandro P, Payne MR** (2016) The predictive skill of species distribution models for plankton in a changing climate. *Global Change Biology* **22**: 3170–3181
- Calbet A, Garrido S, Saiz E, Alcaraz M, Duarte CM** (2001) Annual Zooplankton Succession in Coastal NW Mediterranean Waters: The Importance of the Smaller Size Fractions. *Journal of Plankton Research* **23**: 319–331
- Castellani C, Licandro P, Fileman E, di Capua I, Mazzocchi MG** (2016) *Oithona similis* likes it cool: evidence from two long-term time series. *Journal of Plankton Research* **38**: 703–717
- Choi B-J, Wilkin JL** (2007) The Effect of Wind on the Dispersal of the Hudson River Plume. *Journal of Physical Oceanography* **37**: 1878–1897

- Christou ED** (1998) Interannual variability of copepods in a Mediterranean coastal area (Saronikos Gulf, Aegean Sea). *Journal of Marine Systems* **15**: 523–532
- Cruzado A, Velasquez ZR** (1990) Nutrients and phytoplankton in the Gulf of Lions, northwestern Mediterranean. *Continental Shelf Research* **10**: 931–942
- Cury P, Shannon L** (2004) Regime shifts in upwelling ecosystems: observed changes and possible mechanisms in the northern and southern Benguela. *Progress in Oceanography* **60**: 223–243
- Demarcq H, Wald L** (1984) La dynamique superficielle du panache du Rhône d'après l'imagerie infrarouge satellitaire. *Oceanologica Acta* **7**: 159–162
- Dolédec S, Chessel D, ter Braak CJF, Champely S** (1996) Matching species traits to environmental variables: a new three-table ordination method. *Environ Ecol Stat* **3**: 143–166
- Doray M, Petitgas P, Huret M, Duhamel E, Romagnan JB, Authier M, Dupuy C, Spitz J** (2018a) Monitoring small pelagic fish in the Bay of Biscay ecosystem, using indicators from an integrated survey. *Progress in Oceanography* **166**: 168–188
- Doray M, Petitgas P, Romagnan JB, Huret M, Duhamel E, Dupuy C, Spitz J, Authier M, Sanchez F, Berger L, et al** (2018b) The PELGAS survey: Ship-based integrated monitoring of the Bay of Biscay pelagic ecosystem. *Progress in Oceanography* **166**: 15–29
- Duchon J** (1976) Fonctions-spline et espérances conditionnelles de champs gaussiens. *Annales scientifiques de l'Université de Clermont Mathématiques* **61**: 19–27
- Espinasse B, Carlotti F, Zhou M, Devenon JL** (2014) Defining zooplankton habitats in the Gulf of Lion (NW Mediterranean Sea) using size structure and environmental conditions. *Marine Ecology Progress Series* **506**: 31–46
- Fernández de Puelles ML, Molinero JC** (2008) Decadal changes in hydrographic and ecological time-series in the Balearic Sea (western Mediterranean), identifying links between climate and zooplankton. *ICES Journal of Marine Science* **65**: 311–317
- Feuilloy G, Fromentin J-M, Stemmann L, Demarcq H, Estournel C, Saraux C** (2020) Concomitant changes in the environment and small pelagic fish community of the Gulf of Lions. *Progress in Oceanography* **186**: 102375
- Field null, Behrenfeld null, Randerson null, Falkowski null** (1998) Primary production of the biosphere: integrating terrestrial and oceanic components. *Science* **281**: 237–240
- Fransz HG, Colebrook JM, Gamble JC, Krause M** (1991) The zooplankton of the north sea. *Netherlands Journal of Sea Research* **28**: 1–52
- Frayse M, Pairaud I, Ross ON, Faure VM, Pinazo C** (2014) Intrusion of Rhone River diluted water into the Bay of Marseille: Generation processes and impacts on ecosystem functioning. *Journal of Geophysical Research: Oceans* **119**: 6535–6556
- Frost BW** (1972) Effects of Size and Concentration of Food Particles on the Feeding Behavior of the Marine Planktonic Copepod *Calanus Pacificus*1. *Limnology and Oceanography* **17**: 805–815
- Fullgrabe L, Grosjean P, Gobert S, Lejeune P, Leduc M, Engels G, Dauby P, Boissery P, Richir J** (2020) Zooplankton dynamics in a changing environment: A 13-year survey in the northwestern Mediterranean Sea. *Marine Environmental Research* **159**: 104962
- Garnier E, Lavorel S, Ansquer P, Castro H, Cruz P, Dolezal J, Eriksson O, Fortunel C, Freitas H, Golodets C, et al** (2007) Assessing the Effects of Land-use Change on Plant Traits, Communities and Ecosystem Functioning in Grasslands: A Standardized Methodology and Lessons from an Application to 11 European Sites. *Annals of Botany* **99**: 967–985
- Garrido M, Cecchi P, Vaquer A, Pasqualini V** (2013) Effects of sample conservation on assessments of the photosynthetic efficiency of phytoplankton using PAM fluorometry. *Deep Sea Research Part I: Oceanographic Research Papers* **71**: 38–48

- Gatti J, Petrenko A, Devenon J-L, Leredde Y, Uises C** (2006) The Rhone river dilution zone present in the northeastern shelf of the Gulf of Lion in December 2003. *Continental Shelf Research* **26**: 1794–1805
- Gaudy R, Youssara F, Diaz F, Raimbault P** (2003) Biomass, metabolism and nutrition of zooplankton in the Gulf of Lions (NW Mediterranean). *Oceanologica Acta* **26**: 357–372
- Goberville E, Beaugrand G, Edwards M** (2014) Synchronous response of marine plankton ecosystems to climate in the Northeast Atlantic and the North Sea. *Journal of Marine Systems* **129**: 189–202
- Gohin F, Bryère P, Lefebvre A, Sauriau P-G, Savoye N, Vantrepotte V, Bozec Y, Cariou T, Conan P, Coudray S, et al** (2020) Satellite and In Situ Monitoring of Chl-a, Turbidity, and Total Suspended Matter in Coastal Waters: Experience of the Year 2017 along the French Coasts. *Journal of Marine Science and Engineering* **8**: 665
- Gohin F, Druon JN, Lampert L** (2002) A five channel chlorophyll concentration algorithm applied to SeaWiFS data processed by SeaDAS in coastal waters. *International Journal of Remote Sensing* **23**: 1639–1661
- Gohin F, Loyer S, Lunven M, Labry C, Froidefond J-M, Delmas D, Huret M, Herbland A** (2005) Satellite-derived parameters for biological modelling in coastal waters: Illustration over the eastern continental shelf of the Bay of Biscay. *Remote Sensing of Environment* **95**: 29–46
- Hansen B, Bjornsen PK, Hansen PJ** (1994) The size ratio between planktonic predators and their prey. *Limnology and Oceanography* **39**: 395–403
- Hassett RP** (2004) Supplementation of a diatom diet with cholesterol can enhance copepod egg-production rates. *Limnology and Oceanography* **49**: 488–494
- Hayes K, Sliwa C, Migus S, McEnnulty F, Dunstan P** (2005) National priority pests: Part II Ranking of Australian marine pests. CSIRO Marine Research
- Helenius LK, Saiz E** (2017) Feeding behaviour of the nauplii of the marine calanoid copepod *Paracartia grani* Sars: Functional response, prey size spectrum, and effects of the presence of alternative prey. *PLOS ONE* **12**: e0172902
- Hemingson C, Bellwood D** (2016) Biogeographic patterns in major marine realms: Function not taxonomy unites fish assemblages in reef, seagrass and mangrove systems. *Ecography*. doi: 10.1111/ecog.03010
- Herrmann M, Estournel C, Adloff F, Diaz F** (2014) Impact of climate change on the northwestern Mediterranean Sea pelagic planktonic ecosystem and associated carbon cycle. *Journal of Geophysical Research: Oceans* **119**: 5815–5836
- Huret M, Bourriau P, Doray M, Gohin F, Petitgas P** (2018) Survey timing vs. ecosystem scheduling: Degree-days to underpin observed interannual variability in marine ecosystems. *Progress in Oceanography* **166**: 30–40
- Huret M, Sourisseau M, Petitgas P, Struski C, Léger F, Lazure P** (2013) A multi-decadal hindcast of a physical–biogeochemical model and derived oceanographic indices in the Bay of Biscay. *Journal of Marine Systems* **109–110**: S77–S94
- Ianora A** (1998) Copepod life history traits in subtemperate regions. *Journal of Marine Systems* **15**: 337–349
- Ianora A, Buttino I** (1990) Seasonal cycles in population abundances and egg production rates in the planktonic copepods *Centropages typicus* and *Acartia clausi*. *Journal of Plankton Research* **12**: 473–481
- Jiang Q, Smith RB, Doyle J** (2003) The nature of the mistral: Observations and modelling of two MAP events. *Quarterly Journal of the Royal Meteorological Society* **129**: 857–875
- Josué IIP, Sodr e EO, Setubal RB, Cardoso SJ, Roland F, Figueiredo-Barros MP, Bozelli RL** (2021) Zooplankton functional diversity as an indicator of a long-term aquatic restoration in an Amazonian lake. *Restoration Ecology* **29**: e13365
- Kjørboe T** (2011) How zooplankton feed: mechanisms, traits and trade-offs. *Biological Reviews* **86**: 311–339
- Kjørboe T, Ceballos S, Thygesen UH** (2015) Interrelations between senescence, life-history traits, and behavior in planktonic copepods. *Ecology* **96**: 2225–2235

- Kjørboe T, Visser A, Andersen KH** (2018) A trait-based approach to ocean ecology. *ICES Journal of Marine Science* **75**: 1849–1863
- Kleyer M, Dray S, Bello F, Lepš J, Pakeman RJ, Strauss B, Thuiller W, Lavorel S** (2012) Assessing species and community functional responses to environmental gradients: which multivariate methods? *Journal of Vegetation Science* **23**: 805–821
- Kouwenberg J** (1994) Copepod Distribution in Relation to Seasonal Hydrographics and Spatial Structure in the North-western Mediterranean (Golfe du Lion). *Estuarine Coastal and Shelf Science - ESTUAR COAST SHELF SCI* **38**: 69–90
- Lavorel S, Grigulis K, McIntyre S, Williams NSG, Garden D, Dorrough J, Berman S, Quétier F, Thébault A, Bonis A** (2008) Assessing functional diversity in the field – methodology matters! *Functional Ecology* **22**: 134–147
- Legendre P, Anderson MJ** (1999) Distance-Based Redundancy Analysis: Testing Multispecies Responses in Multifactorial Ecological Experiments. *Ecological Monographs* **69**: 1–24
- Legendre P, Legendre L** (2012) *Numerical Ecology*. Elsevier
- Litchman E, Ohman MD, Kjørboe T** (2013) Trait-based approaches to zooplankton communities. *Journal of Plankton Research* **35**: 473–484
- Lochet F, Leveau M** (1990) Transfers between a eutrophic ecosystem, the river Rhône, and an oligotrophic ecosystem, the north-western Mediterranean Sea. *Hydrobiologia* **207**: 95–103
- Lombard F, Koski M, Kjørboe T** (2013) Copepods use chemical trails to find sinking marine snow aggregates. *Limnology and Oceanography* **58**: 185–192
- Macias D, Garcia-Gorriç E, Stips A** (2018) Deep winter convection and phytoplankton dynamics in the NW Mediterranean Sea under present climate and future (horizon 2030) scenarios. *Sci Rep* **8**: 6626
- Martini S, Larras F, Boyé A, Faure E, Aberle N, Archambault P, Bacouillard L, Beisner BE, Bittner L, Castella E, et al** (2021) Functional trait-based approaches as a common framework for aquatic ecologists. *Limnology and Oceanography* **66**: 965–994
- Masse J, Uriarte A, Angelico M, Carrera P** (2018) Pelagic survey series for sardine and anchovy in ICES subareas 8 and 9 — Towards an ecosystem approach. ICES cooperative research report. doi: 10.17895/ices.pub.4599
- Millot C** (1990) The Gulf of Lions' hydrodynamics. *Continental Shelf Research* **10**: 885–894
- Millot C, Taupier-Letage I** (2005) Circulation in the Mediterranean Sea. *In* A Salot, ed, *The Mediterranean Sea*. Springer, Berlin, Heidelberg, pp 29–66
- Molinero JC, Ibanez F, Souissi S, Buecher E, Dallot S, Nival P** (2008) Climate control on the long-term anomalous changes of zooplankton communities in the Northwestern Mediterranean. *Global Change Biology* **14**: 11–26
- Nicolas D, Rochette S, Llope M, Licandro P** (2014) Spatio-Temporal Variability of the North Sea Cod Recruitment in Relation to Temperature and Zooplankton. *PLOS ONE* **9**: e88447
- Nowaczyk A, Carlotti F, Thibault-Botha D, Pagano M** (2011) Distribution of epipelagic metazooplankton across the Mediterranean Sea during the summer BOUM cruise. *Biogeosciences* **8**: 2159–2177
- Nygaard B, Ejrnæs R** (2004) A new approach to functional interpretation of vegetation data. *Journal of Vegetation Science* **15**: 49–56
- Palmer MW, McGlenn DJ, Westerberg L, Milberg P** (2008) Indices for Detecting Differences in Species Composition: Some Simplifications of Rda and Cca. *Ecology* **89**: 1769–1771
- Petitgas P, Doray M, Huret M, Massé J, Woillez M** (2014) Modelling the variability in fish spatial distributions over time with empirical orthogonal functions: anchovy in the Bay of Biscay. *ICES Journal of Marine Science* **71**: 2379–2389

- Petitgas P, Goarant A, Massé J, Bourriau P** (2009) Combining acoustic and CUFES data for the quality control of fish-stock survey estimates. *ICES Journal of Marine Science* **66**: 1384–1390
- Pielou EC** (1966) The measurement of diversity in different types of biological collections. *Journal of Theoretical Biology* **13**: 131–144
- Pisano A, Marullo S, Artale V, Falcini F, Yang C, Leonelli FE, Santoleri R, Buongiorno Nardelli B** (2020) New Evidence of Mediterranean Climate Change and Variability from Sea Surface Temperature Observations. *Remote Sensing* **12**: 132
- Pomerleau C, Sastri AR, Beisner BE** (2015) Evaluation of functional trait diversity for marine zooplankton communities in the Northeast subarctic Pacific Ocean. *Journal of Plankton Research* **37**: 712–726
- Poulsen LK, Kiørboe T** (2005) Coprophagy and coprorhexy in the copepods *Acartia tonsa* and *Temora longicornis*: clearance rates and feeding behaviour. *Marine Ecology Progress Series* **299**: 217–227
- Price JF, Weller RA, Pinkel R** (1986) Diurnal cycling: Observations and models of the upper ocean response to diurnal heating, cooling, and wind mixing. *Journal of Geophysical Research: Oceans* **91**: 8411–8427
- Qiu Z, Doglioli AM, Carlotti F** (2009) Zooplankton transport and distributions in the Gulf of Lions: Estimates from a Lagrangian model and optical remote sensing data. 2009 IEEE International Geoscience and Remote Sensing Symposium. p II-468-II-471
- Raven JA, Falkowski PG** (1999) Oceanic sinks for atmospheric CO₂. *Plant, Cell & Environment* **22**: 741–755
- Regimbart A, Guitton J, Le Pape O** (2018) Zones fonctionnelles pour les ressources halieutiques dans les eaux sous souveraineté française. Deuxième partie : Inventaire.
- Richardson AJ** (2008) In hot water: zooplankton and climate change. *ICES Journal of Marine Science* **65**: 279–295
- Richardson AJ, Schoeman DS** (2004) Climate Impact on Plankton Ecosystems in the Northeast Atlantic. *Science* **305**: 1609–1612
- Richirt J, Goberville E, Ruiz-Gonzalez V, Sautour B** (2019) Local changes in copepod composition and diversity in two coastal systems of Western Europe. *Estuarine, Coastal and Shelf Science* **227**: 106304
- Roman MR** (1984) Utilization of detritus by the copepod, *Acartia tonsa*1. *Limnology and Oceanography* **29**: 949–959
- R Core Team** (2021). R: A language and environment for statistical computing. R Foundation for Statistical Computing, Vienna, Austria. URL <https://www.R-project.org/>.
- Rose M** (1933) Copépodes pélagiques. Librairie de la faculté des sciences de Paris
- Pinca and Dallot** (1995) Meso- and macrozooplankton composition patterns related to hydrodynamic structures in the Ligurian Sea (Trophos-2 experiment, April-June 1986). *Marine Ecology Progress Series* **126**: 49–65
- Sadaoui M, Ludwig W, Bourrin F, Raimbault P** (2016) Controls, budgets and variability of riverine sediment fluxes to the Gulf of Lions (NW Mediterranean Sea). *Journal of Hydrology* **540**: 1002–1015
- Sarmiento JL, Hughes TMC, Stouffer RJ, Manabe S** (1998) Simulated response of the ocean carbon cycle to anthropogenic climate warming. *Nature* **393**: 245–249
- Schminke HK** (2007) Entomology for the copepodologist. *Journal of Plankton Research* **29**: i149–i162
- Shannon CE** (1948) A mathematical theory of communication. *The Bell System Technical Journal* **27**: 379–423
- Shepard D** (1968) A two-dimensional interpolation function for irregularly-spaced data. Proceedings of the 1968 23rd ACM national conference. Association for Computing Machinery, New York, NY, USA, pp 517–524

- Sicre M-A, Jalali B, Martrat B, Schmidt S, Bassetti M-A, Kallel N** (2016) Sea surface temperature variability in the North Western Mediterranean Sea (Gulf of Lion) during the Common Era. *Earth and Planetary Science Letters* **456**: 124–133
- Simpson EH** (1949) Measurement of Diversity. *Nature* **163**: 688–688
- Siokou-Frangou I, Christaki U, Mazzocchi MG, Montresor M, Ribera d’Alcalá M, Vaqué D, Zingone A** (2010) Plankton in the open Mediterranean Sea: a review. *Biogeosciences* **7**: 1543–1586
- Stoecker DK, Egloff DA** (1987) Predation by *Acartia tonsa* Dana on planktonic ciliates and rotifers. *Journal of Experimental Marine Biology and Ecology* **110**: 53–68
- Taylor AH** (2002) 1 North Atlantic climatic signals and the plankton of the European Continental Shelf. *In* K Sherman, HR Skjoldal, eds, *Large Marine Ecosystems*. Elsevier, pp 3–26
- Turner JT** (2015) Zooplankton fecal pellets, marine snow, phytodetritus and the ocean’s biological pump. *Progress in Oceanography* **130**: 205–248
- Violle C, Navas M-L, Vile D, Kazakou E, Fortunel C, Hummel I, Garnier E** (2007) Let the concept of trait be functional! *Oikos* **116**: 882–892
- Wackernagel H** (1995) Ordinary Kriging. *In* H Wackernagel, ed, *Multivariate Geostatistics: An Introduction with Applications*. Springer, Berlin, Heidelberg, pp 74–81
- Ware DM, Thomson RE** (2005) Bottom-Up Ecosystem Trophic Dynamics Determine Fish Production in the Northeast Pacific. *Science* **308**: 1280–1284
- Yebra L, Espejo E, Putzeys S, Giráldez A, Gómez-Jakobsen F, León P, Salles S, Torres P, Mercado JM** (2020) Zooplankton Biomass Depletion Event Reveals the Importance of Small Pelagic Fish Top-Down Control in the Western Mediterranean Coastal Waters. *Frontiers in Marine Science* **7**: 1155
- (2008) Directive 2008/56/EC of the European Parliament and of the Council of 17 June 2008 establishing a framework for community action in the field of marine environmental policy (Marine Strategy Framework Directive) (Text with EEA relevance).

APPENDICES

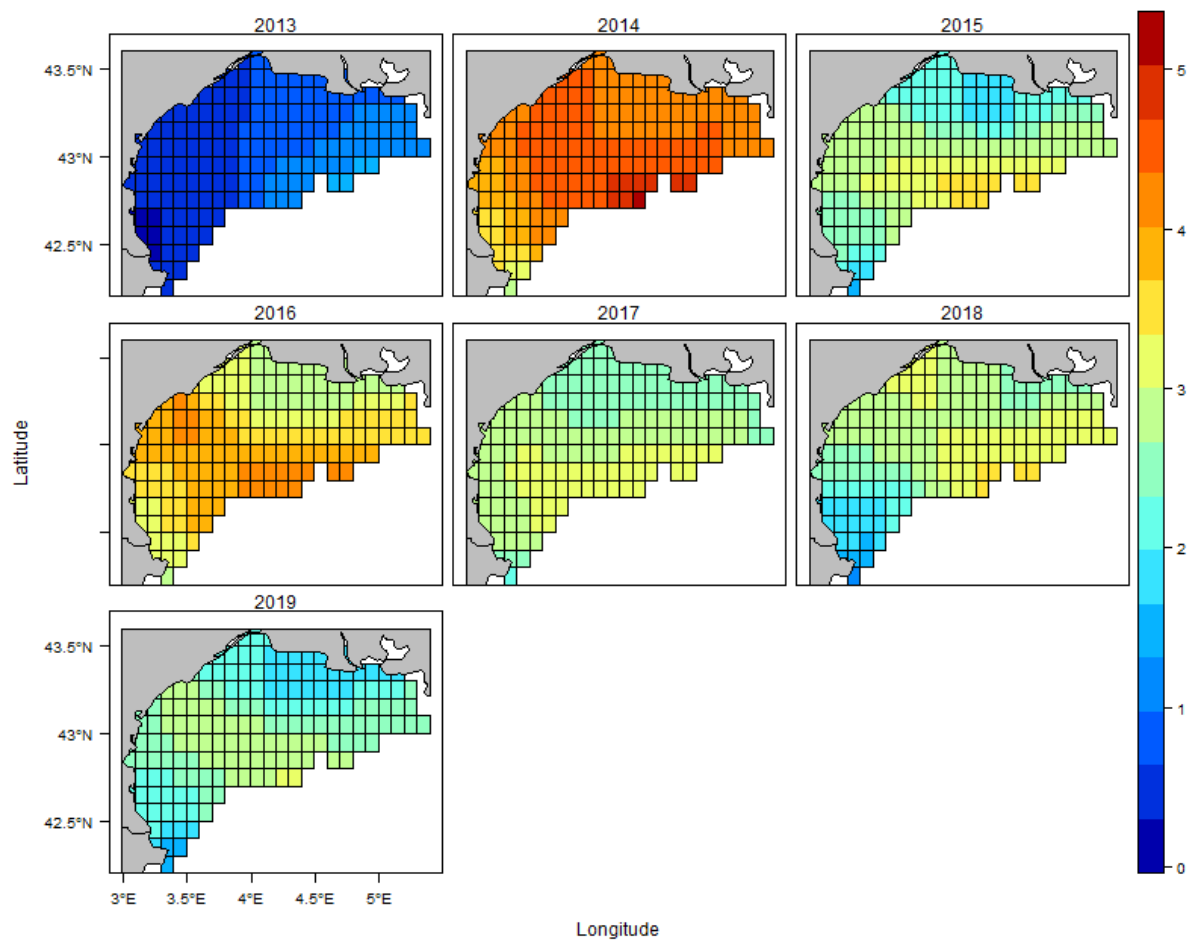
Appendix 1 Table : Review of kriging methods (principle, pros and cons) tested to map copepod abundance from PELMED surveys.

Method	Principle	Advantages and drawbacks	Application to PELMED data	References and R packages used
Ordinary kriging ^a	Estimate a point, for which a variogram is known, using data in the neighborhood	-Simple -Most used -Sensitive to sampling design	No because too influenced by sampling protocol AND not enough points to fit a good variogram. Mean variogram could not be used.	Automap package Wackernagel (1995)
Inverse distance weighting (IDW)	Estimates cell values by averaging the values in the neighbourhood. Points closer have more weight.	-Minimize RMSE -Choose the best method -Do not use variograms	No - due to the heterogeneity of the maps	Dorado package gstat package Shepard (1968)
Nearest neighbourhood	A value is assigned to a certain grid cell from the nearest observation.	BUT		gstat package

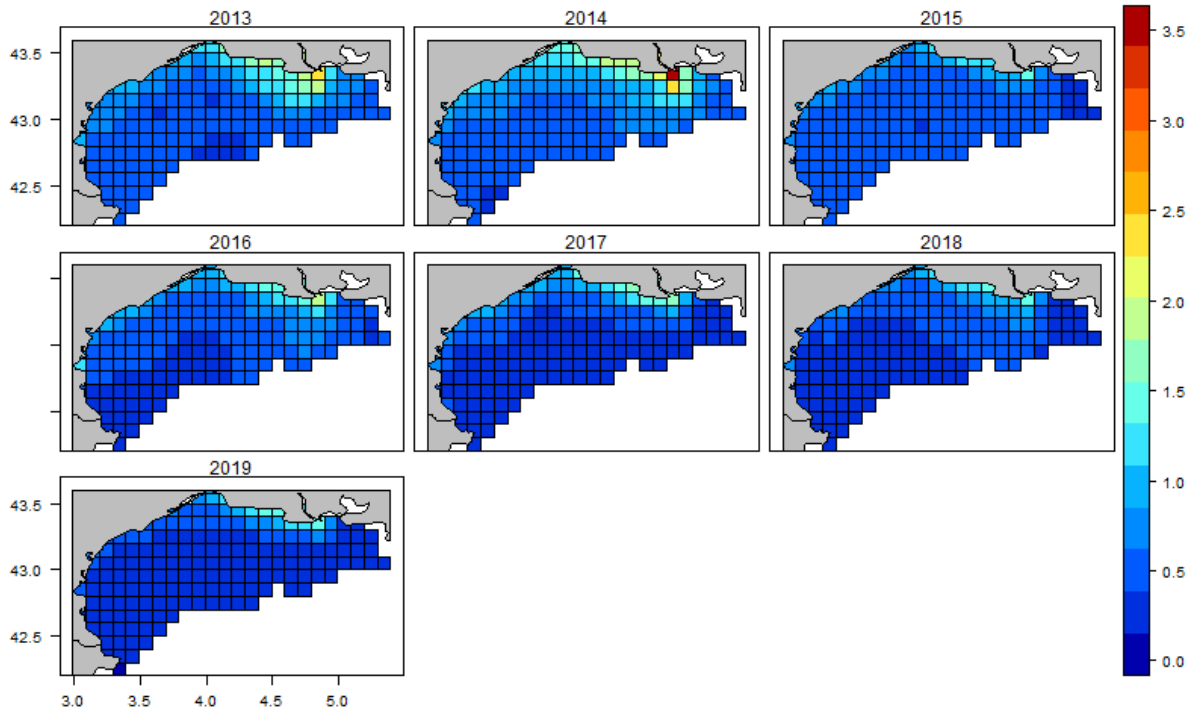
Thin Plate Spline Regression (TPS)	Spline-based technique for data interpolation and smoothing	-Heterogeneous maps, difficult to compare		Fields package Duchon (1976)
Block averaging	Data are averaged by block over a grid	Simple procedure used for other sampling survey of there same type (e.g. fish) Does not use a variogram. Suitable to a heterogenous sample design. Suitable to cover large areas.	Yes	Petitgas et al. (2009, 2014) Package EchoR and the function gridNplot

a: This method was combined to the block averaging method in specific cases (see text for details)

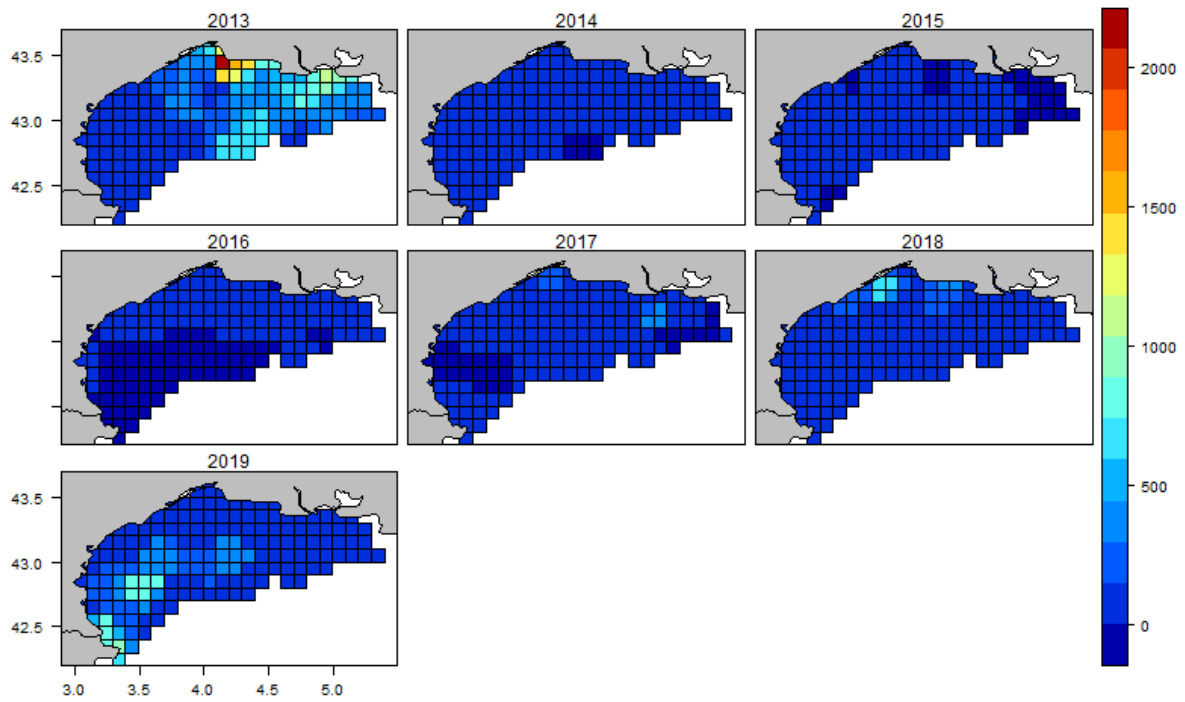
APPENDIX 2: Maps of wind speed in July in $\text{m}\cdot\text{s}^{-1}$ during PELMED survey from 2013 to 2019



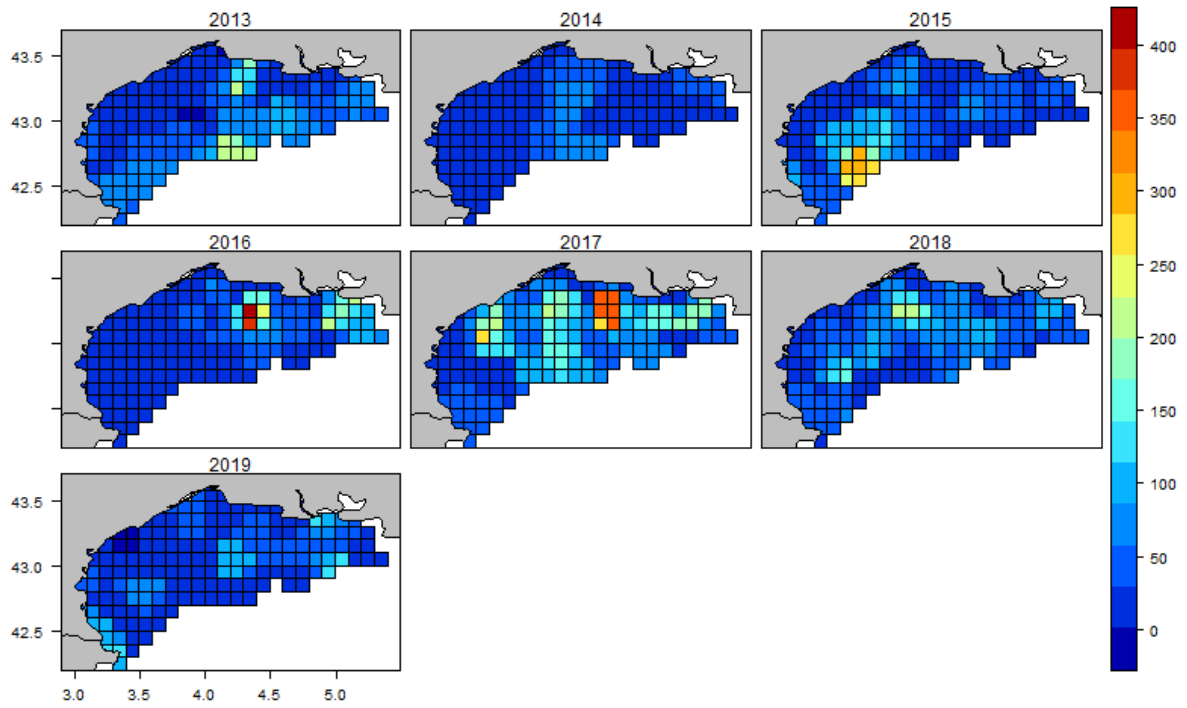
APPENDIX 3: Maps of turbidity in mg.m^{-3} during PELMED survey from 2013 to 2019



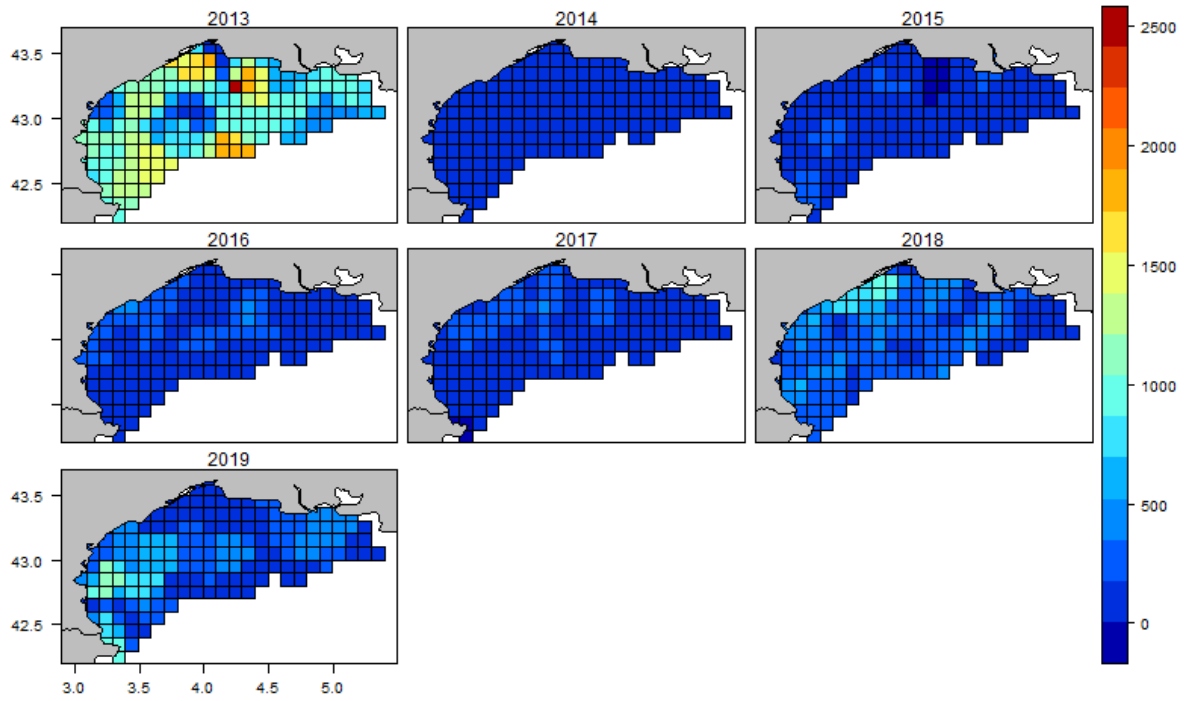
APPENDIX 4: Map of abundance (ind.m⁻³) of *Acartia clausi* during PELMED surveys from 2013 to 2019



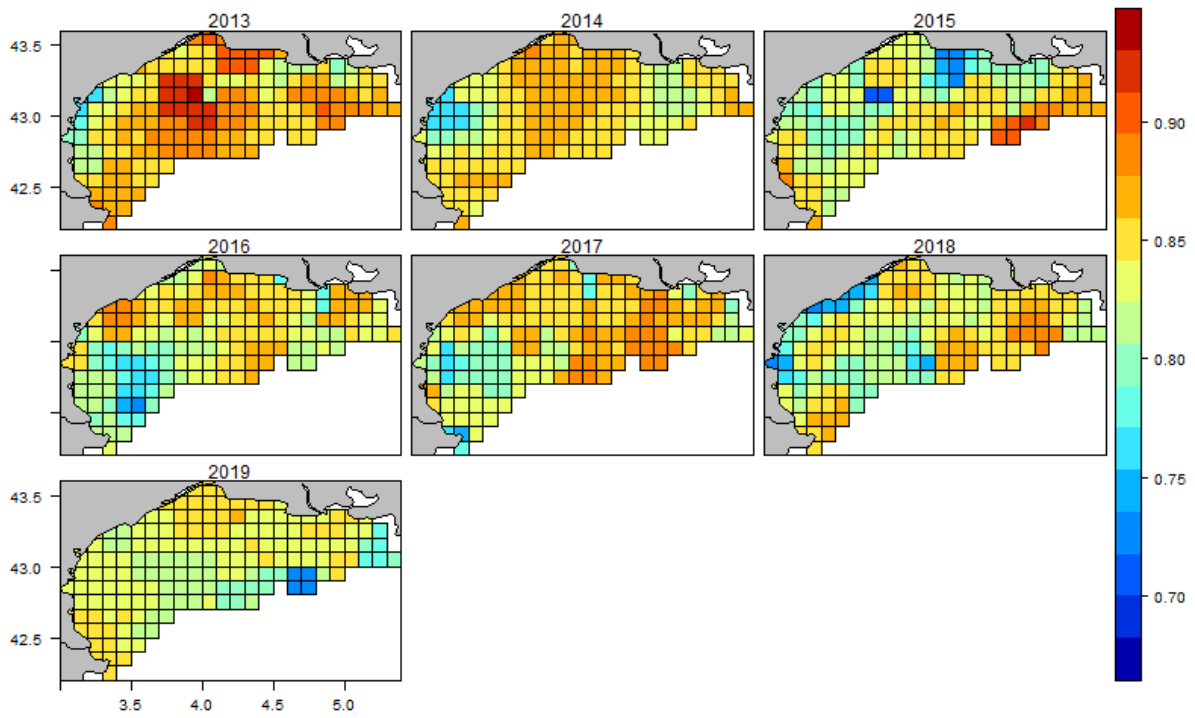
APPENDIX 5: Map of abundance (ind.m⁻³) of *Centropages typicus* during PELMED surveys from 2013 to 2019



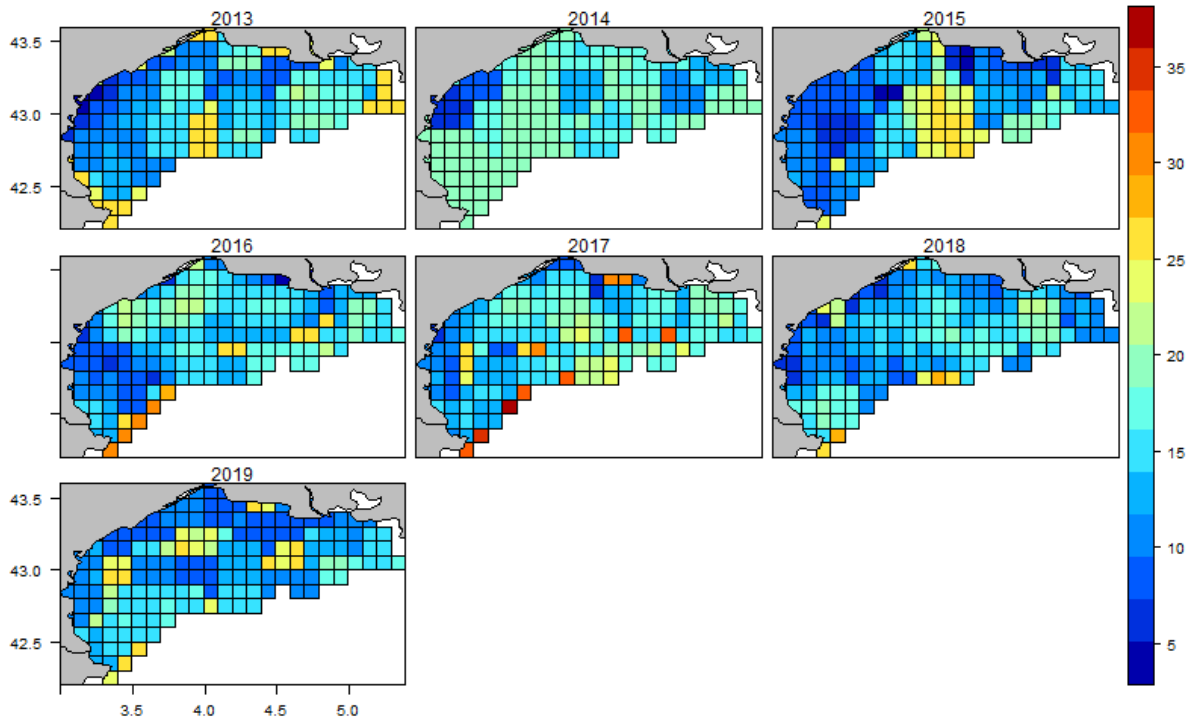
APPENDIX 6: Map of abundance (ind.m⁻³) of *Oithona similis* during PELMED surveys from 2013 to 2019



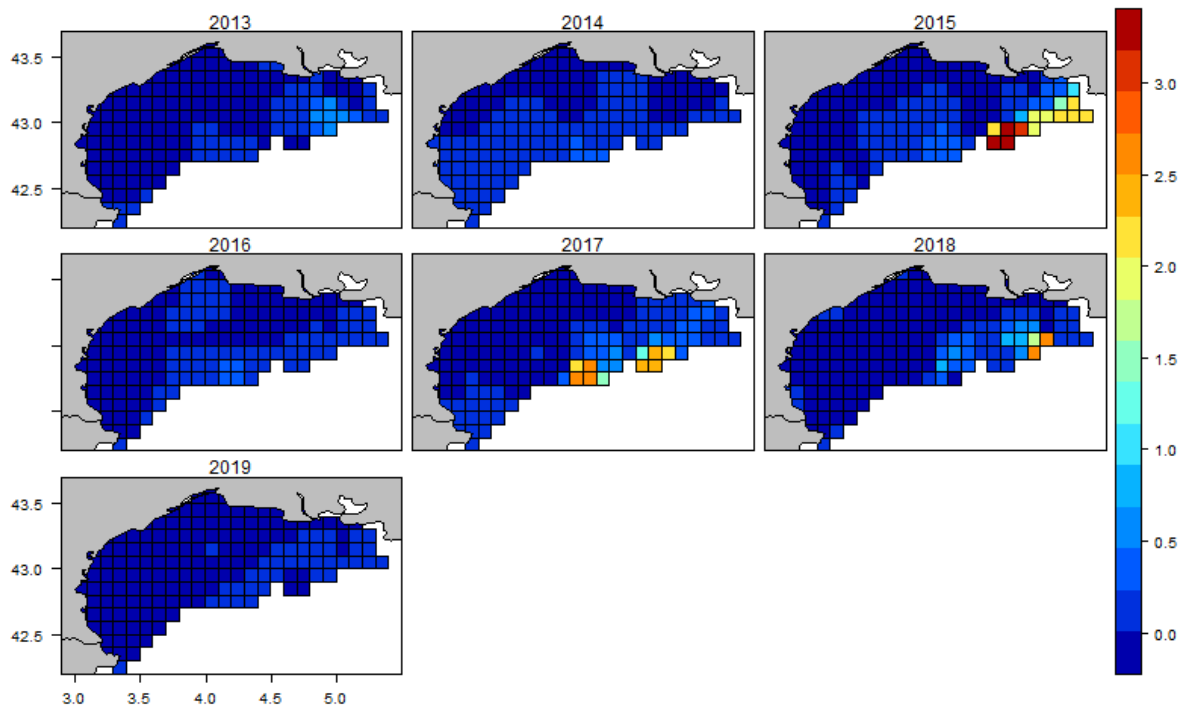
APPENDIX 7 : Simpson diversity index of copepod during PELMED surveys from 2013 to 2019.



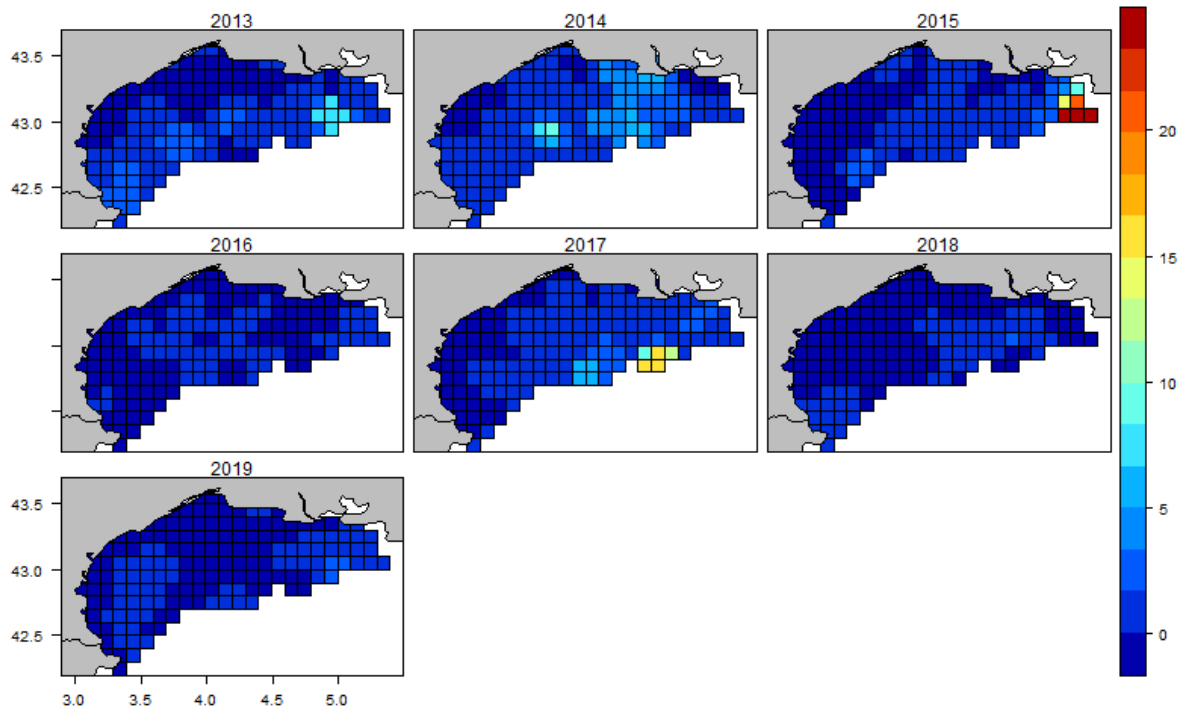
APPENDIX 8: Species richness index during PELMED surveys from 2013 to 2019



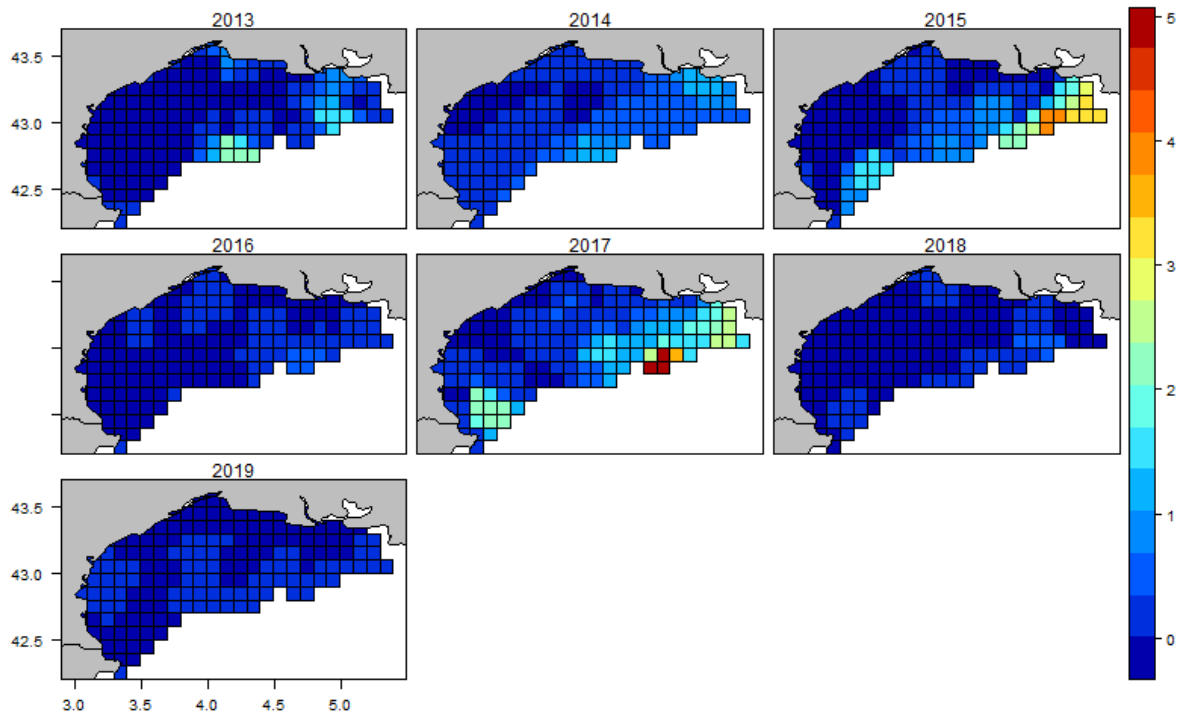
APPENDIX 9: Map of abundance (ind.m⁻³) of *Heterorhabdus pappiliger* during PELMED surveys from 2013 to 2019



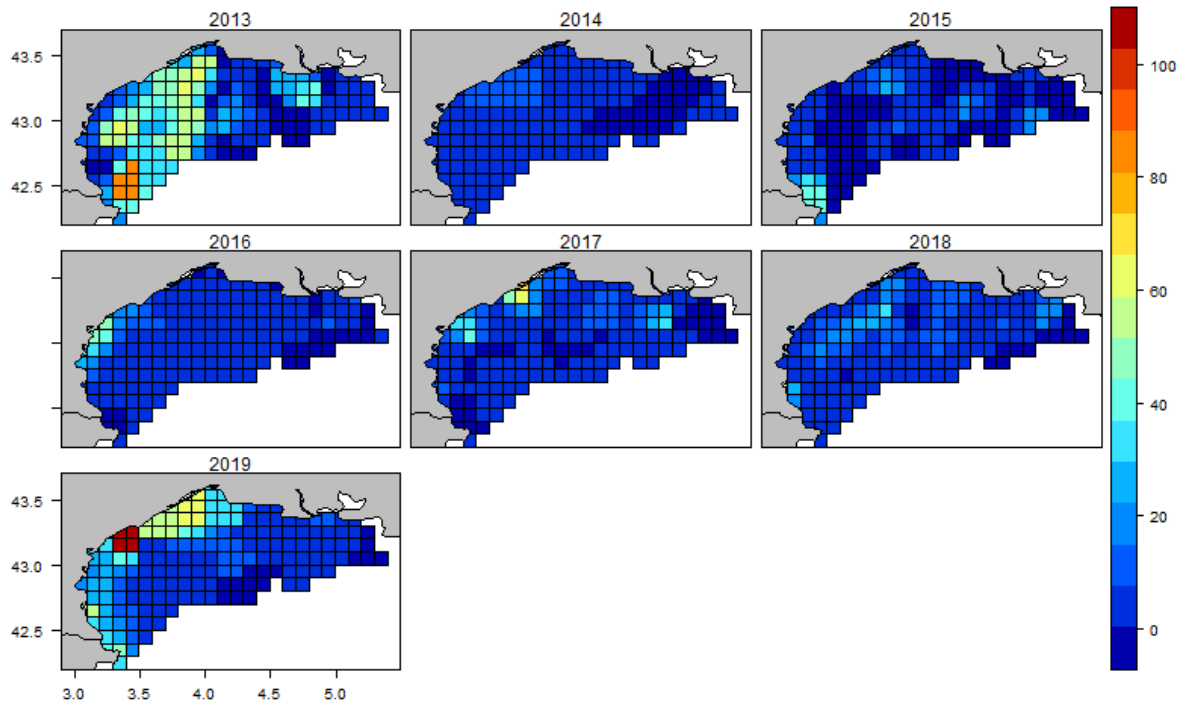
APPENDIX 10: Map of abundance (ind.m⁻³) of *Pleurommama gracilis* during PELMED surveys from 2013 to 2019



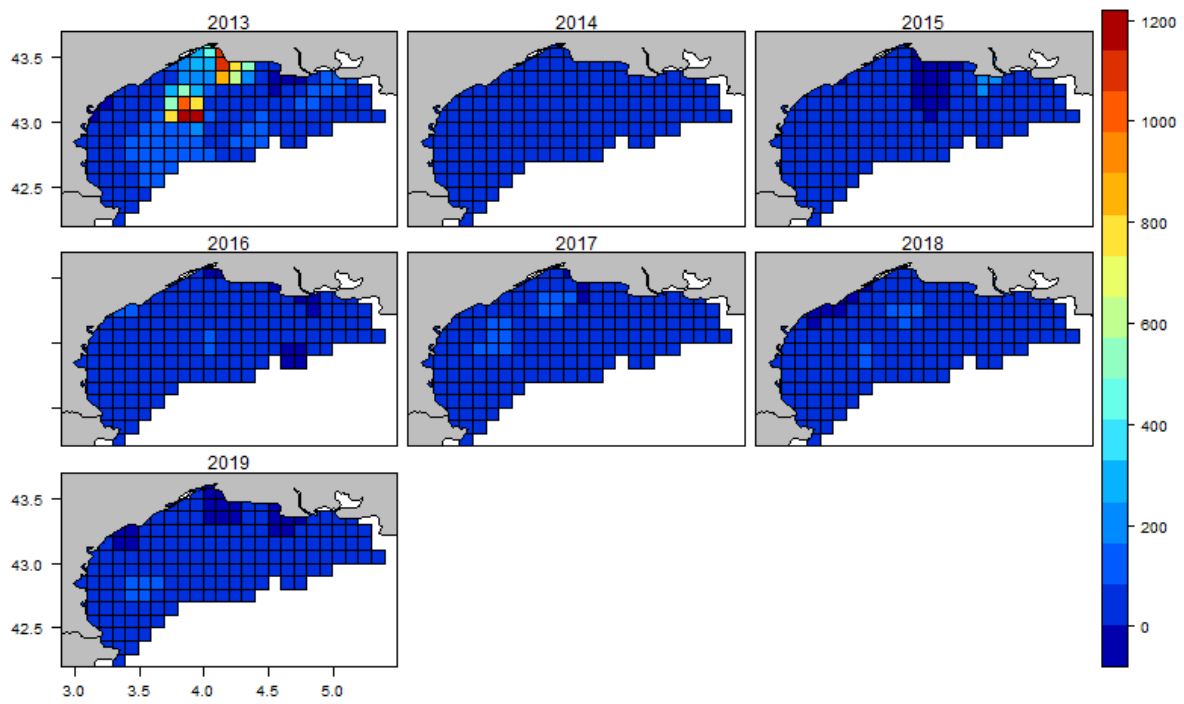
APPENDIX 11: Map of abundance (ind.m⁻³) *Nannocalanus minor* during PELMED survey from 2013 to 2019



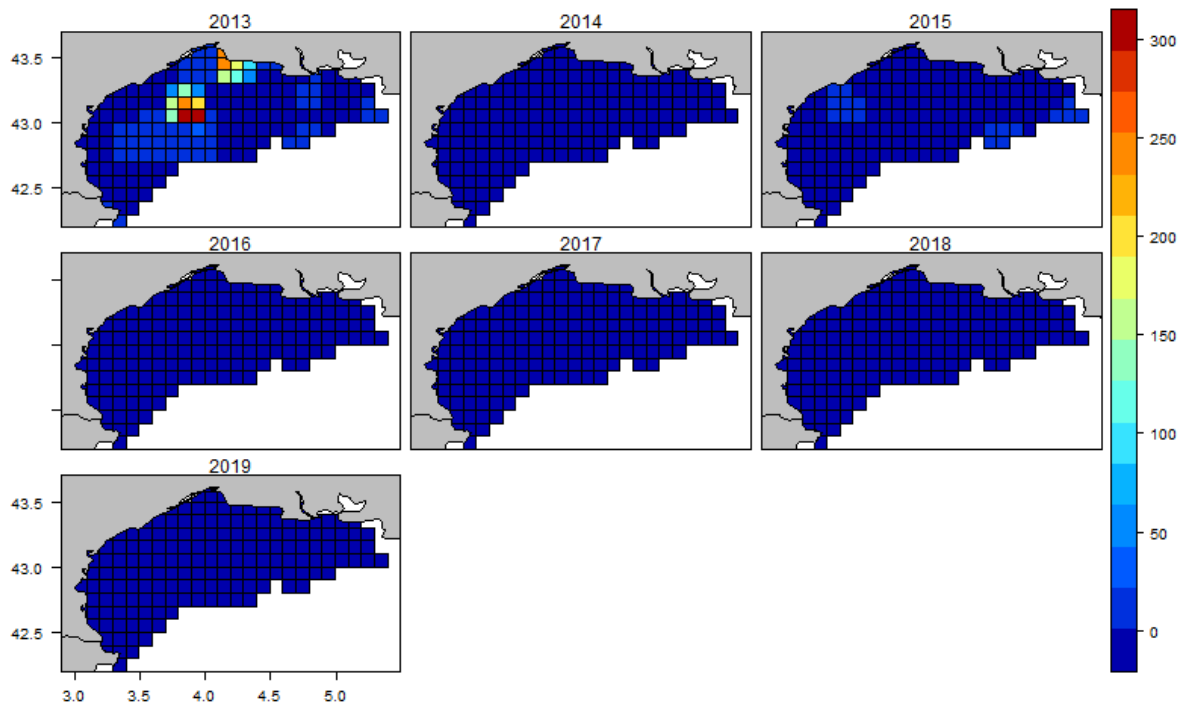
APPENDIX 12: Map of abundance (ind.m⁻³) of *Oithona nana* during PELMED surveys from 2013 to 2019



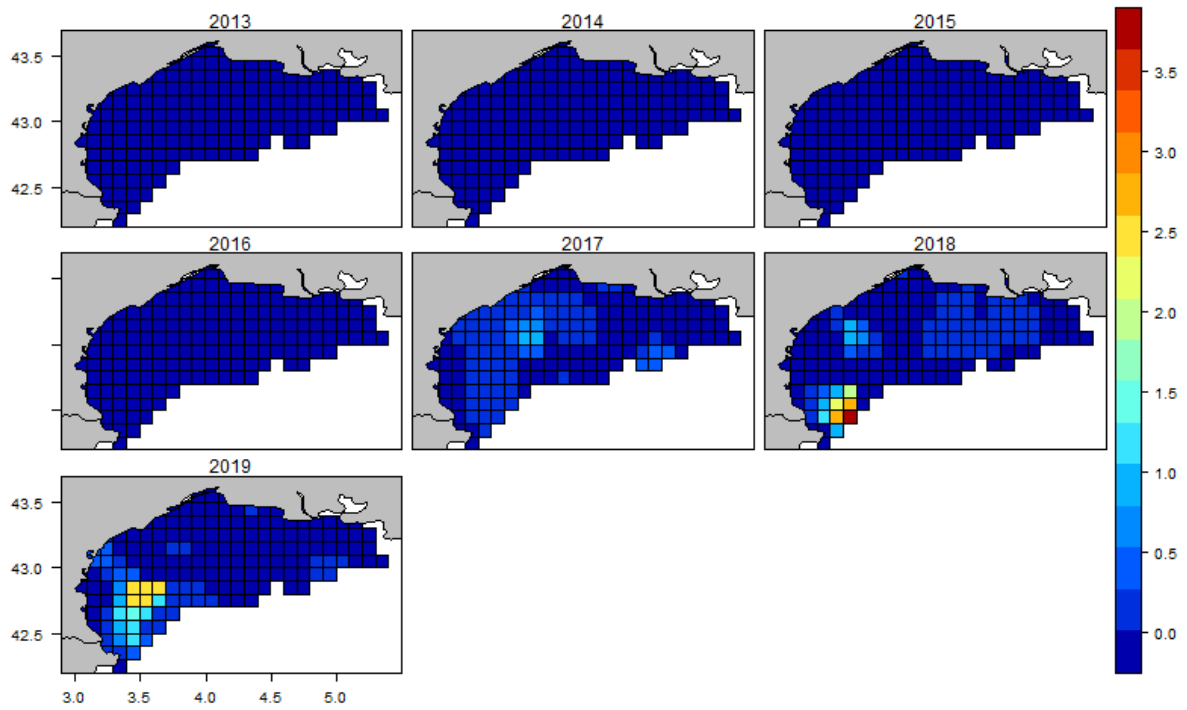
APPENDIX 13: Map of abundance (ind.m⁻³) of *Oithona plumifera* during PELMED surveys from 2013 to 2019



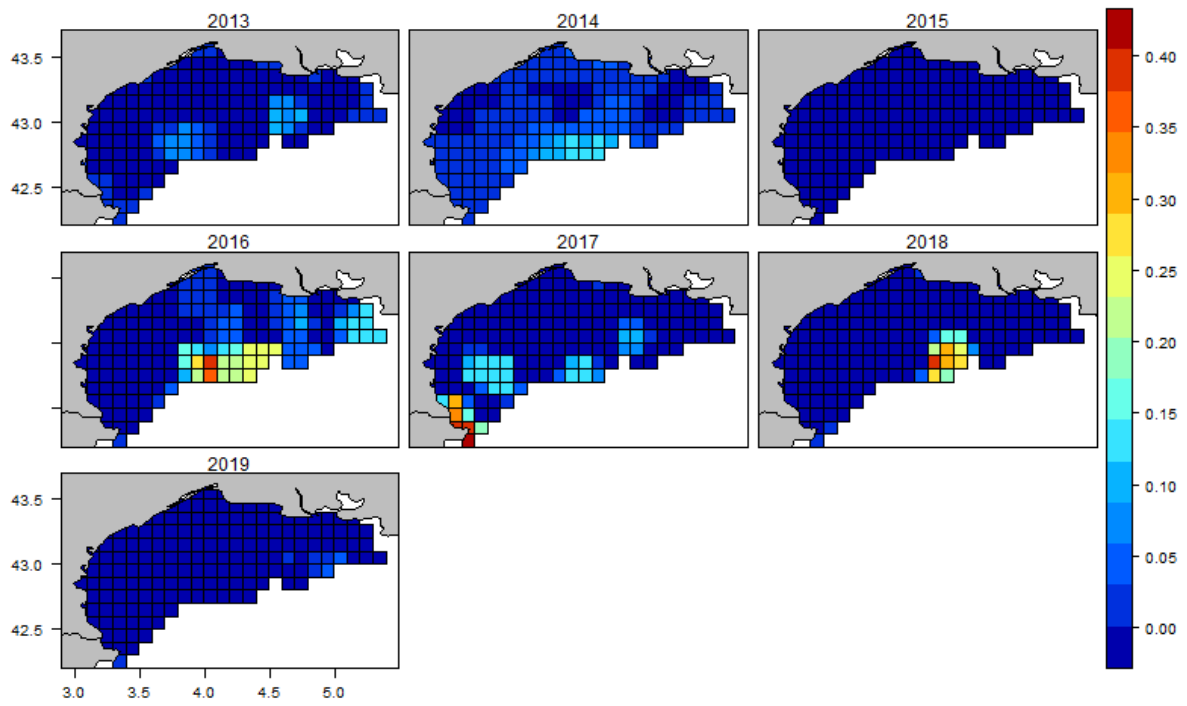
APPENDIX 14: Map of abundance (ind.m⁻³) of *Oithona setigera* during PELMED surveys from 2013 to 2019




APPENDIX 15:Map of abundance (ind.m⁻³) of *Diaxis pygmaea* during PELMED survey from 2013 to 2019



APPENDIX 16: Map of abundance (ind.m⁻³) of *Haloptilus longicornis* during PELMED survey from 2013 to 2019



 agriculture • alimentation • environnement	Diplôme : Ingénieur agronome Spécialité : Agronome Spécialisation / option : Sciences halieutiques et aquacoles – Ressources et Ecosystèmes Aquatiques Enseignant référent : Olivier LE PAPE
Auteur(s) : Amélie Nithard Date de naissance* : 30/12/1997	Organisme d'accueil : UMR MARBEC Sète Adresse : Avenue Jean Monnet 34200 Sète
Nb pages : 35 Annexe(s) : 16	Maître de stage : Tarek Hattab et Dorothee Vincent
Année de soutenance : 2021	
Titre français : gradients de variabilité spatiale et inter-annuelle de la diversité taxinomique et fonctionnelle du zooplancton dans le golfe du Lion	
Titre anglais : spatial and inter-annual variability gradients of zooplanktonic taxonomic and functional diversity in the gulf of Lion	
<p>Résumé : Cette étude apporte une première analyse exploratoire et quantitative des données zooplanctoniques issues de PELMED afin d'étudier la distribution du zooplancton en été sur une période de 7 ans (2013-2019) dans le Golfe du Lion. Le block averaging (méthode de cartographie) a été utilisé afin de représenter la variabilité spatiale et temporelle des abondances, des groupes fonctionnels et taxinomiques. La variabilité environnementale a aussi été cartographiée et explorée par analyse en coordonnées principales. Se concentrant sur les communautés de copépodes, une analyse de redondance (RDA) a été appliquée aux valeurs des traits moyens des communautés et ainsi qu'aux données environnementales et a permis d'identifier (i) les groupes fonctionnels et taxinomiques les plus sensibles aux changements environnementaux et (ii) les forçages responsables de la variabilité observée. Les résultats de ces travaux font apparaître des gradients environnementaux marqués (côte-large et est-ouest) impactant la structure et la distribution des communautés de copépodes. La variabilité interannuelle observée est surtout due à la stratification des eaux, induite par les événements hydrologiques (température, salinité, vents) et permet d'identifier deux fonctionnements distincts de l'écosystème planctonique estival. A la côte, les traits fonctionnels des copépodes et les variables environnementales (Chl-a, matières en suspension) suggère l'existence d'une réseau trophique basée sur des ressources phytoplanctoniques et détritiques alimentant des copépodes herbivores/omnivores essentiellement localisés dans la zone épipélagique. Au large, la colonne d'eau est fortement stratifiée, occupée par des organismes de grandes tailles localisés dans les couches profondes (e.g. <i>C. typicus</i>). Les résultats sont discutés d'un point de vue méthodologique, écologique et les perspectives de ces travaux en Méditerranée sont envisagées en termes de surveillance.</p>	
<p>Abstract : Zooplankton communities are considered as good indicators of environmental changes and could be used to monitor marine ecosystems. The standardized and optimized surveys within the EU MSFD, which include the integrated pelagic ecosystem survey PELMED, aims to collect the data needed to assess the state of the marine environment. In this study we carried out the first numerical and exploratory analyses of the zooplankton dataset collected during the PELMED survey to study the distribution patterns of summer zooplankton communities over a 7-year period (2013-2019) in the gulf of Lion. Block averaging (mapping method) has been used to represent the spatial and temporal variability of taxonomic and functional composition of zooplankton, with a focus on copepod communities. Environmental variability has also been mapped and explored using a PCoA ordination method. Then a redundancy analysis applied to community-weighted mean functional traits and environmental data has been used to identify which functional or taxonomic group was more sensitive to changes in environmental conditions and which environmental forcing was responsible. Our analyses revealed strong environmental gradients from the coast to the oceanic region offshore and from the west to the east. The distribution of the zooplankton community and their functional traits seem to be related to the spatial and temporal variability of the considered environmental conditions. Interannual variability has been observed within zooplankton communities, mainly due to the stratification of the waters induced by hydrological events (wind, temperature, salinity). Identifying the functional groups and zooplankton communities living in stratified waters is a prerequisite for the development of good environmental state indicators within the MSFD, but more data and analyses are needed.</p>	
Mots-clés : copepodes – trait fonctionnel – variabilité - Méditerranée	
Key Words: copepods – functional trait – variability – Mediterranean	

* Élément qui permet d'enregistrer les notices auteurs dans le catalogue des bibliothèques universitaires